2005

AN ORGANIC BOVINE HYDROXYAPATITE-PLGA COMPOSITES FOR BONE TISSUE ENGINEERING

Harini Raman
University of Kentucky

ABSTRACT OF THESIS

ANORGANIC BOVINE HYDROXYAPATITE-PLGA COMPOSITES FOR BONE TISSUE ENGINEERING

The objective of the present study was to synthesize porous, biodegradable poly (D, l-lactide-co-glycolide) PLGA-B-HA (Bovine hydroxyapatite) composite and evaluate the effect of ceramic content on bone marrow cell differentiation *in vitro*. A macroporous biodegradable PLGA-B-HA composite with the pore size varying from 0.1 to 1000μ and a highly interconnected structure was fabricated using the freeze-drying/lyophilization technique. A pilot study was done to determine the effects of B-HA on to the osteoblast function. The main study was done to determine the effect of the increase in B-HA concentration on to the mesenchymal stem cell differentiation. Morphological characteristics of the composites were analyzed using FTIR and SEM/EDX analysis. The composites were seeded with neonatal rat calvarial osteoblasts (NRCO). The polymer: ceramic ratio in this study was 35%:65%. For comparison parallel experiments involving pure HA-200 discs were performed. SEM results indicated a higher proliferation and mineralization on PLGA-B-HA composites than pure HA discs. In addition, we evaluated the *in vitro* characteristics of PLGA-B-HA composites with varying ratios, i.e., 1:1, 1:2 and 1:3, seeded with rat marrow cells. FTIR indicated an increase in the area under the ceramic peak as ceramic concentration was increased. In addition, the average roughness values increased in the order of 1:3 > 1:2 > 1:1. Both compressive strength and modulus of 1:1 were significantly higher than 1:2 and 1:3 PLGA-B-HA composites. No significant difference in compressive modulli and strengths could be observed for 1:2 and 1:3 PLGA-B-HA composites. Cellular activity was determined by measuring AP activity, total protein analysis and osteocalcin concentration. Evaluation of alkaline phosphatase activity showed bone cells attached to 1:3 (PLGA-B-HA) expressed significantly higher alkaline phosphatase as compared to 1:1 and 1:2 PLGA-B-HA composites. In addition, cells seeded on to 1:3 composites secreted significantly higher osteocalcin and at a relatively short time period as compared to the other samples. Corrosion studies (ICP) and pH values indicate minimal difference in the concentration of Ca and P and pH in tissue culture media for all the samples at the end of all time periods. Hence we conclude that an increase in the ceramic concentration stimulated mesenchymal stem cell differentiation thereby promoting osteogenesis.

KEYWORDS: neonatal rat calvarial osteoblasts, freeze drying, mesenchymal stem cells, bovine hydroxyapatite, osteogenesis

Harini Raman

06/02/05

ANORGANIC BOVINE HYDROXYAPATITE-PLGA COMPOSITES FOR BONE TISSUE ENGINEERING

By

Harini Raman

Dr. Ahmed El-Ghannam
Director of Thesis

Dr. Abhijit Patwardhan
Director of Graduate Studies

06/02/05

RULES FOR THE USE OF THESES

Unpublished theses submitted for the Master's degree and deposited in the University of Kentucky Library are as a rule open for inspection, but are to be used only with due regard to the rights of the authors. Bibliographical references may be noted, but quotations or summaries of parts may be published only with the permission of the author, and with the usual scholarly acknowledgements.

Extensive copying or publication of the thesis in whole or in part also requires the consent of the dean of the Graduate School of the University of Kentucky. A Library that borrows this thesis for use by its patrons is expected to secure the signature of each user.

THESIS

Harini Raman

The Graduate School

University of Kentucky

2005

ANORGANIC BOVINE HYDROXYAPATITE-PLGA COMPOSITES FOR BONE TISSUE ENGINEERING

THESIS

A thesis submitted in partial fulfillment of the requirements for the degree of Master of Science in the Graduate School at the University of Kentucky

By

Harini Raman

Advisor: Dr. Ahmed El-Ghannam

Lexington, Kentucky

June 2005

MASTER'S THESIS RELEASE

I authorize the University of Kentucky
Libraries to reproduce this thesis in whole or part
for purpose of research

Signed: _____

Date: _____

ACKNOWLEDGEMENTS

I would like to thank and extend my gratitude to my advisor and professor, Dr. Ahmed El-Ghannam and Dr. David A. Puleo. Their guidance, support and perseverance through the course of my research were invaluable. I am thankful to them for having offered me such an incredible opportunity. Without their assistance I would not have earned this valuable degree. I would also like to thank Dr. Jie Cai who helped me begin my research at the University. .

I would like to thank Dr. Conquin Ning, Junaid Mehta and Gautam Gupta for assisting me in certain areas of research.

I would like to thank Dr. Scott Stephens for letting me use their laboratory equipment for surface roughness measurements. I would like to thank Sriram Venkatesan for assisting me with the "New View 5000". I would like to thank Larry Rice for helping me with the SEM.

Appreciation is also extended to Dr. Charles Knapp, member of the thesis committee, for his support and encouragement throughout my degree.

And finally to my mother and father who worked so arduously for me to get here.

TABLE OF CONTENTS

LIST OF FIGURES

Pilot study

Main study

LIST OF TABLES

CHAPTER ONE

INTRODUCTION

1.1 Motivation

Medical procedures relevant to bone related injuries prevalent in the United States with over 800,000 grafting procedures are done annually [1]. 10% of the bone grafting procedures include the use of synthetic graft substitutes. There is a need to develop effective bone substitutes to heal large bone defects due to trauma; congenital disorders etc. Autografts are tissues taken from the same patient. They are widely in the form of cancellous autogenous bone or the gold standard [2]. They are osteogenic, osteoconductive and osteoinductive. The presence of surviving cells, osteoinductive proteins i.e. bone matrix proteins, mineralized matrix, and collagen supports cell function. The limitations include donor site morbidity which includes pain, due to grafting and limited availability of the donor organs. The procedure is expensive and may be associated with post surgery complications.

Allografts on the other hand are bone graft substitutes that include tissue taken from a different patient. The limitations include risk of infection during transplantation process. It may also be accompanied with inflammatory reactions and in extreme cases leads to graft rejection [2-4]. One case of hepatitis B transmission and 3 cases of hepatitis C transmission have been reported with allograft tissue; the latest case occurred in 1992. Cases involving HIV transmission have been reported in 2000 [2]. Xenografts include transplantation of cells from different species. As with allografts, the major problem is related with biocompatibility issues, humans have "natural antibodies" that circulate in

the blood and cause immediate graft rejection when organs from some species are transplanted (for example grafts made from pig organs) [4].

Biomaterials based on polymers, ceramics, metals, bioactive glasses and composites materials are used as synthetic bone graft substitutes [1-3, 5-7]. The limitations that metals possess include extremely high mechanical properties than bone thereby leading to stress shielding, subsequent weakening of the host tissue and making it susceptible to fracture. The challenges currently include fabricating a biocompatible substrate that provides a surface promoting direct bone apposition that ultimately acts as the true bone tissue. Donor organ scarcity limits the number of people who require organ transplantation. This problem has urged the development of a substrate that restores the function of damaged tissue and enhances reconstruction using the tissue engineering approach. The advantages of this technique include the elimination of repeated surgery at the donor site.

The tissue engineered scaffolds must provide 3-dimensional tissue growth providing optimal growth space and vascularization. In addition the scaffolds should be biocompatible, highly porous and must have non-toxic degradation products. High porosity provides sufficient space to promote cell infiltration within the scaffolds. The viability of the cells would be maintained by vascularization. The cell viability is hindered if the vascularization is improper which is dependent upon the interconnected porous network structure of the scaffold [5].

1.2 Autologous transplants involving bone marrow stem cells

In an organism formation of bone takes place during the development of embryo, growth, remodeling, fracture repair, and when induced experimentally for e.g. by purified or recombinant members of the bone morphogenetic family (BMP). Bone marrow stroma contains cells that have both proliferative and differentiative capacity. The differentiative ability of the cells enables them to form multiple lineages, e.g. bone, cartilage, marrow adipocytes, fibrous tissue and any other tissue in the body. This ability of unlimited and extensive regenerative ability is due to regeneration of marrow stroma [8].

The mesenchymal stem cells differentiation into respective osteoblastic lineage or from osteoblastic progenitors to an osteoblast starts with multipotential stem cells with an unlimited regenerative capacity. The differentiation of multipotential stem cells leads to the formation of progenitors for other mesenchymal cells including adipocytes, fibroblasts and myoblasts as well as precursors for osteoblasts. They divide further to form immature and then mature osteoprogenitors. At this stage these cells have limited self regenerative capacity but high rate of proliferation. The mature progenitors differentiate to form prosteoblasts which further differentiate into mature osteoblasts. The mature osteoblasts divide post mitotically and give rise to osteocytes and eventually leading to apoptosis. As the osteoblastic lineage progresses the cells have a limited rate of proliferation but an extensive rate of differentiation. This continues till the cells differentiate to form mature osteoblasts and which further differentiate to form osteocytes [8].

Variety of materials have been researched and incorporated to heal osseous defects. These include autogenous and allogenic tissues [8-11]. While surgeons have extensively used autograft to deliver osteoblasts to defect sites, the transplantation of *in vitro* expanded osteoprogenitor cells is one of the current areas of focus in research today. *In vitro* cultured human mesenchymal stem cells can synthesize collagenous and noncollagenous proteins that are the components of skeletal matrix. A promising approach involves the transplantation of human bone marrow stem cells (BMSC's), which have been shown to possess a high osteogenic potential. In order to make BMSC transplantation useful as a method for forming new bone to close osseous defects in patients, the technique must be improved to optimize the rate, extent of proliferation and mechanical strength of the newly formed bone [8].

The development of a suitable matrix that permits the growth of the newly forming bone or provides a surface that promotes direct bone apposition is a current focus of research. A macroporous structure of the matrix permits extensive vascularization from the host tissue and promotes cell viability and function. This further allows the transplant to be incorporated in the defect region. This characteristic of the carrier matrix stimulates the differentiation of mesenchymal stem cells to their specific osteoblast phenotype [9-10].

Osteogenic cells derived from rat bone marrow cells were cultured on polymeric two-dimensional and three-dimensional tissue engineered scaffolds. The results indicated that the scaffolds supported osteoblast function by the formation of a mineralized matrix directly on the polymer surface. This bone-like apatite layer formed on the surface of the

substrate promotes cell attachment and proliferation thereby allowing direct bone bonding. The mineralized layer stimulates osteoblasts to secrete collagenous matrix [11].

1.3 Ideal Bone Graft substitute

The properties of an ideal bone graft substitute include simulating an autograft but eliminating the problems associated with it. The scaffold when implanted within the body should be biocompatible and bioresorbable with non-toxic degradation by products. It should be composed of an osteoconductive matrix that mimics the calcified matrix of the tissue and/or contains necessary bioactive factors to make it osteoconductive. This includes autogenous osteoblast transplantation on to biodegradable, bioresorbable and porous scaffolds. Porosity enables the infiltration of the cells deep within the scaffolds and maintains cell viability by promoting vascularization. The transplanted cells may secrete new matrix and factors necessary for bone ingrowth while the bioresorbable material gradually degrades [9-11].

1.4 Types of Composites used as Bone substitutes

Composite materials have been widely used in bone reconstruction procedures. They include polymer-ceramic composites, polymers composites of PLA, PGA, PLGA, PLLA, PDLA, polyurethanes and polycaprolactones etc. or ceramic composites of calcium phosphate series that include monocalcium and bi-calcium phosphates, α and β-tricalcium phosphates, hydroxyapatite and bioactive glass composites etc. Polymers have good mechanical strength but they lack osteoconductivity, on the other hand ceramics are osteoconductive but are brittle [1-10, 26, 31, 42]. To address the limitations of individual

materials, new materials based on composites of ceramics and polymers have been proposed.

1.4.1 Polymers

1.4.1.1 Properties

Biodegradable polymers have been observed to support mesenchymal stem cell differentiation and in cartilage regeneration [4-7]. Copolymers of two α-polyesters i.e. polylactic acid (PLA) and polyglycolic acid (PGA) have been widely used to their inherent biodegradable properties. They enhance bone remodeling by transferring mechanical load to the surrounding tissues by virtue of degradation. They can be completely resorbed within the body and can be eliminated by the normal metabolic processes.

The degradation rates of copolymers could range from days to years by varying the ratio of lactic acid to glycolic acid. Implants comprising of 100% PLA or 100% PGA degrade at a slower rate than the copolymers due to their high crystallinity. The polymer degradation is due to hydrolysis. A crystalline morphology provides a definite structure that restricts the penetration of water molecules thereby lowering the degradation rate. Since the half life of PGA is shorter than that of PLA; hence increasing the PGA content will enhance the degradation process. Other factors that influence the degradation rate include viscosity and molecular weight of copolymers. Higher the molecular weight and viscosity, slower would be the degradation as compared to low viscosity and low molecular weight polymers [7].

1.4.1.2 Applications

1.4.1.2.1 Drug delivery

Biodegradable polymers such as poly (DL-lactide-co-glycolide) (PLGA) and polylactides (PLA) are widely used for drug delivery due to their controlled degradation and biocompatibility within the host tissues. [12]. In addition the major advantages of biodegradable drug delivery systems involving hydrolyzing polymers is the elimination of reoperation rates. The degradation by products are non toxic and can be eliminated by the body easily which may not be the case for polymers like polyurethanes etc [12-13]**.**

The distribution of the encapsulated drug within the polymeric phase would be influenced by drug's solid-state solubility and by the ability of the polymeric matrix to entrap drug in dispersed state. An increase in the lactide content leads to the increase in hydrophobicity and facilitates relatively higher solubility of a hydrophobic drug within the hydrophobic phase. The release of drug is governed by its separation from the polymeric phase and the surrounding aqueous environment. Higher the solubility of the drug within the polymeric matrix, lower is the separation of the drug from the polymer to the external aqueous phase. This results in lower rates of drug release. The drug release from the biodegradable polymers i.e. PLGA/PLA polymers in the form of nano and microparticles comprises of an initial controlled release phase followed by a slow release period and a second release phase, which is characterized by the bulk degradation of the polymer matrix [12, 14-15].

1.4.1.2.2 In Bone regeneration

Several studies have shown use of PLGA as a scaffold to induce new bone tissue formation [1, 3-11, 13, 17]. The advantages of using PLGA as a scaffold for bone regeneration include 1) fabricated in different shapes; 2) the degradation time, mechanical strength, and flexibility can be easily modulated by altering the copolymer ratio; 3) even distribution of the cells throughout the scaffold thereby enhancing osteogenesis throughout the system.

1.4.2 Calcium Phosphate ceramics

1.4.2.1 Properties

Calcium phosphate ceramics have been widely used in tissue engineering applications due to the following reasons; a) they have a chemical composition similar to the inorganic component of bone; b) have high CaO contents and have been reported to have good bioactivity, and the osteoblasts can readily form mineral deposits on the surfaces of CP's *in vitro* and *in vivo*; c) induces the formation of bone like apatite layer thereby providing direct bone bonding on to the surface unlike non bioactive materials. The resorption rates of calcium phosphate ceramics have been studied widely. Resorption rate of calcium phosphate ceramics depended on the form, chemical composition, porosity (macro and micro), dissolution in the environment and cell mediated resorption. [16, 18-21]. Resorption of calcium phosphates promoted bone formation [20, 25-26]. The free Ca^{+2} ions released in the surrounding environment during the dissolution process have been shown to induce bioactivity [22, 24-25].

1.4.2.1.1 Comparison of resorption rates of the calcium phosphate ceramics on osteogenesis

Dissolution and precipitation reactions occurring on the surface of calcium phosphate ceramics leads to the formation of an apatite layer that would stimulate osteoblast migration and function. Yuan et al. observed more bone ingrowth at the end of 150 days within the porous β- TCP, whereas no bone in growth could be observed in the case of α-TCP at the same time period [26]. Higher porosity facilitates dissolution/precipitation and thereby mediating cell migration and function. Differences in bone formation could be attributed to the differences in dissolution rates of the ceramics. β- TCP resorbs at a slower rate as compared to α-TCP. But at longer time *in vivo*, β- TCP becomes more resorbable. Dissolution/precipitation reactions at the ceramic-media interface results in the formation of a bone-like apatite layer that promotes otseogenesis. Higher dissolution of the ceramic for e.g. i.e. α-TCP could cause an increase in the local concentration of Ca^{+2} and PO_4^{-3} thereby resulting in an increase in the local pH that may be unfavorable to the surrounding environment. This may further hinder bone formation. Lower dissolution of the ceramic reduces leads to decreased bioactivity as in the case of β –TCP thereby hindering the already formed new bone on to the implant surface. Degradation of ceramics could be altered depending upon the type and structure of the ceramic that is being used thereby affecting the new bone formation.

1.4.2.1.2 Effect of varying porosity of calcium phosphate ceramics on osteogenesis

Effects of varying the sintering temperature onto the morphology of different ceramics were studied. deGroot et al. investigated the influence of surface modifications on the osteoconductive properties of two types of calcium phosphate ceramics (HA and β- TCP) [31]. HA was sintered at 1150 and 1250^0 C. β- TCP consisted a blend of β- TCP and HA was sintered at 1100, 1150 and 1200^0 C. The results indicated that changes in sintering temperatures did not influence the ceramic chemistry and the blend composition. Increasing the sintering temperature resulted in a decrease in microporosity with macroporosity not being affected. An increase in microporosity within a macroporous structure increases the specific surface area available for cell material interactions thereby triggering the cells to differentiate into the osteoblastic phenotypes.

1.4.2.2 Applications

1.4.2.2.1 As cell-based carriers

Ti carriers have been used as because of their biocompatibility and excellent mechanical properties [27-30]. Ti-fiber mesh implants and ceramic implants (60% HA and 40% α-TCP) were incorporated with rat bone marrow stem cells and implanted subcutaneously. New bone formation at the end of 1, 3 and 6 weeks in the case of ceramics grew up by 18% as compared to Ti-fiber meshes which grew up by 10%. Calcium phosphate ceramics could be designed as a carrier system so as to deliver cells in the host site due to significantly higher bone formation as compared to Ti implants.

1.4.2.2.2 As a carrier of Bone morphogenetic protein

Calcium phosphate ceramics were investigated *in vitro* and *in vivo* as a delivery system for bone morphogenetic proteins to induce bone formation in soft tissues. The significance of BMP in calcium phosphate ceramics has been evaluated [32]. *In vitro* experiments, studies have shown that BMP mixed with calcium phosphate ceramics can induce rapid bone formation [33-34] and the bone formation was significantly higher than that of BMP alone [33]. Enhancement of bone formation was seen in calcium phosphate ceramics incorporated with b-BMP (Bovine-BMP). It was observed that the b-BMP from the b-BMP solution *in vitro* was not only absorbed on to the calcium phosphate ceramics and but it also adsorbed native BMP from *in vivo* fluids [32]. This shows a significant role of BMP in calcium phosphate ceramics in osteoinduction. The native BMP adsorption from the *in vivo* body fluids would induce osteogenesis by calcium phosphate ceramics.

1.4.2.2.3 As a bone graft substitute in intervertebral spinal fusion

Calcium phosphate ceramic composites incorporated with mesenchymal stem cells provide an alternative to autogenous graft materials for lumbar interbody spinal fusion. Efficacy of bone marrow stem cells seeded on to calcium phosphate ceramics as bone graft substitutes in a lumbar intervertebral spinal fusion process in rabbits were studied [35].

1.4.3 Polymer-Ceramic composites (Bone substitute composites)

1.4.3.1 Properties

The advantages of combining a biodegradable polymer (PLGA) with a ceramic (HA) are used in tissue regeneration due to the following reasons, Improved mechanical properties of the composite, enhanced osteoconductive properties of the polymer and due to the buffering action on the acidic degradation byproducts from polyesters. Hydoxyapatite ceramics are least soluble as compared to other CP ceramics. Due to its stability and controlled degradation rate it could be used *in vivo* to give sufficient time to heal the defect stimulating simultaneous degradation in a controlled manner [36-37, 41-45]. Bone grafting materials may produce bone formation by osteogenesis, osteoinduction, osteoconduction or osteotransduction. Osteogenesis is a process that includes provision of osteogenic cells and matrix directly on to the graft; osteoinduction implies that the chemotaxicity of the grafted material attracts the undifferentiated osteoprogenitor cells in the host to the site of the graft and stimulates them to differentiate in to osteoblasts, e.g. the use of bone morphogenetic protein; osteoconduction is a process that permits outgrowth of osteogenic cells from existing bone surfaces into adjacent graft material e.g. Calcium phosphate ceramics etc; and osteotransduction involves replacing a bone substitute directly by bone [51].

1.4.3.1.1 Effect of varying the pore size

Pore size is one major factor that controls the osteoblast proliferation or function in vitro. For bone ingrowth, an optimum pore size of 200-400 microns has been observed. Pore size 200-400 μm provides optimal compression and tension on the osteoblast's mechanoreceptors thereby promoting osteoblast function. This property stimulates extracellular matrix secretion by the osteoblasts thereby inducing osteogenesis [36].

1.4.3.1.2 Mechanical properties

Mikos et al. studied hydroxyapatite reinforced poly (α-hydroxy ester) foams for bone regeneration [37]. In this study low- and high-porosity composite foams PLGA and short fiber hydroxyapatite ceramics were synthesized using the solvent casting particulate leaching method. Incorporation of HA increased the compressive yield strengths of both poly (α-hydroxy ester) foams [41-43].

1.4.3.2 Applications

1.4.3.2.1 As a carrier of bone morphogenetic protein

Polymer-ceramic composites were developed as carrier systems to deliver bioactive molecules at targeted region to enhance osteogenesis [38-40]. Miki et al. evaluated osteoinductive potential of PLGA/HA incorporated with BMP-2 in skull defects of rats. Post implantation studies showed that the discs completely resorbed after 4 weeks and the defect was filled with new bone. In contrast composites incorporated in defects without BMP-2 were filled with fibrous connective tissue.

1.4.3.2.2 In Bone regeneration

Besides their osteoconductive effect, ceramics have shown to neutralize the acidic degradation products of PLA thereby improving the biocompatibility of the polymer [26, 31, 41-42]. Therefore their presence would be effective particularly during the degradation of the polymer [41-42]. Most importantly *in vitro* culture studies showed that cell survival percentage on the PLLA-HA (polymer-ceramic) scaffolds significantly improved over the pure PLLA scaffolds. Calcium hydroxyapatite ceramics (CHA) are nontoxic materials and cause minimal inflammatory reaction [44]. When the porous composites were implanted into a rabbit femoral condyle, bone and bone marrow with extensive vasculature formed deep in pores through the interpore connections. Excellent interconnectivity enables osteoconduction thereby promoting cells and tissues to migrate deep in to the pores.

1.5 Fabrication methods/Processing Methods for porous scaffolds

Various methods involving fabrication of low density porous polymeric scaffolds have been synthesized by methods including solution casting/salt leaching, solvent evaporation technique, freeze immersion, phase separation, gel casting, emulsion freeze drying, gas foaming and fiber binding meshes. Solvent evaporation techniques typically produce sacffolds exhibiting smaller pore sizes (1-20 μm). Solvent casting particulate leaching method creates desirable pore size ranges by incorporation of the porogen; sieved NaCl or soluble sugar particles of a desired size. The pore size and the porosity are determined by the particle size and number of particles of the porogen within the polymer. However, the significant loss of hydrophillic bioactive agents (e.g. drugs, antibiotics, growth factors

incorporated into the foam during the fabrication process would occur during the leach-out process [45-48].

1.5.1 Freeze drying/Lyophilization technique

1.5.1.1 Processing Parameters

Several studies have indicated the synthesis of macroporous scaffolds possessing a desired pore range and interconnected porous network [47-49]. Processing parameters included solvent composition, polymer concentration, freezing temperature, polymer type and polymer molecular weight were optimized to arrive at a desired microstructure with an interconnected network that would promote cellular growth and tissue integration.

As the freezing temperature increases, the nucleation rate increases and this results in the formation of large number of small crystals of the solvent. And rapid evaporation of the solvent leads to the formation of a microporous structure. Hence the microporosity can be controlled by the quenching rate of the solvent. Also the solvent/non solvent ratio is also an important determinant for obtaining a three-dimensional interconnected network. Increasing the non solvent concentration leads to the formation of loose polymer particulates with weak strengths were obtained. Porosity decreased by doubling the polymer concentration. Very low polymer concentrations resulted in producing structures with low mechanical strengths [47-49]. The porosity and density of the foams depend on the molecular weight of the polymer chosen. Ma et al. showed that the density of the PLGA-HA foams increased with the increase in the polymer to ceramic ratio [49]. At the same time the porosity decreased as the polymer and the ceramic content were increased.

As the polymer concentration was increased (2.5% to 7.5%), foams with thicker pore walls and high mechanical strengths were obtained. As the polymer concentration was decreased there was a suspension of the HA particles settled within the polymer particles thereby forming a non-uniform solution [49].

1.5.1.2 Coarsening effect

Coarsening (coalescence of the phase separated droplets) continuously proceeds to reduce the free energy associated with the interfacial area [50]. Macroporous scaffolds could be obtained using the coarsening effect, which induces enlargement of the pores. The coarsening time decreased with the increasing quenching temperature (temperature to which the samples were exposed).

The coarsening effect was predominant in the core of the structures resulting in a microporous structure than the surface thereby resulting in a macroporous surface. Increasing the amount of water in the solvent mixture tended to generate large cellular pores. This could be due to the fact that as the non solvent volume increases, a weaker polymer-solvent interaction occurs which might induce the formation of poor phase with greater solvent droplet domains. Increasing the quenching temperature induces the coarsening effect thereby leading to the formation of enlarged pores with closed cellular structures. As the amount of water incorporated into the solvent mixture was increased closed cellular macropores upto 1000 μm were obtained [50].

1.6 Objective/Purpose of the present study

The broad goal of this project is to synthesize porous resorbable bioactive B-HA-Polymer composite that can be used as a tissue engineering scaffold to deliver bone marrow cells. The objective of the present study is to synthesize a porous, biodegradable PLGA- B-HA composite and evaluate the effect of ceramic content on bone marrow cell differentiation *in vitro*. The synthesized macroporous polymer-ceramic scaffold with an interconnected porous network eventually would enhance bone marrow stem proliferation and differentiation in to osteoblastic phenotypes that can be used in treating bone defects.

We have used deproteinized bovine bone hydroxyapatite (B-HA) for the study. Studies have shown that, it is a safe and a biocompatible bone graft material [53] and is of osteoconductive nature [51, 53]. It is obtained from two different bone types, cortical and cancellous bone and commercially available in two particle sizes 0.25-1 mm and 1-2 mm [51]. The PLGA-B-HA composites were fabricated using the freeze drying/solid-liquid phase separation technique. The study was done in order to determine the effect of increase in ceramic concentration on osteoblast activity. Polymer used for the study is Poly-D, L-lactide-co-glycolide (50:50) with a molecular weight 50-70,000 Da. This polymer was chosen due to its controlled degradation 6 months- 1year. The polymers can be tailored to degrade between weeks to years depending upon their copolymer ratio, which can be used to balance the rate of osteoblast growth and ECM deposition on to the degradation rate of the material.

CHAPTER TWO

MATERIALS AND METHODS

2.1 Preparation of Polymer/Hydroxyapatite mixture

Deproteinized bovine hydroxyapatite (B-HA) was prepared and used for the study. The structure of the B-HA was confirmed by X-ray diffraction analysis. Bovine Hydroxyapatite (B-HA) particles were sifted in the size range ($20 < x < 38$) microns. Poly (D, L-lactic-co-glycolic acid, lactide:glycolide ratio 50:50 (PLGA) with IV (Intrinsic viscosity) = 0.58 and Mw = 50,000-70,000 Da (Sigma, St. Louis, MO). The scaffolds were prepared using the freeze drying/Lyophillization techniques. Bovine bone was sintered at 1000^0 C to evaporate the organic material. After the evaporation of the organic matrix, the residual matrix is the porous inorganic matrix which was used for the study. The B-HA ceramic particles were first crushed and sifted to obtain the particle range ($20 < x < 38$) μm. 0.73g of the polymer was mixed with 1.2g of sifted B-HA particles in a 25 ml centrifuge tube followed by the addition of 8ml of chloroform. The solution was allowed to stand for 24 hours for complete dissolution of the polymer. The mixture was vortexed for 5-6 minutes till the polymer was dissolved completely so as to obtain a uniform suspension of the ceramic particles within the polymer solution. The mixture was transferred in to glass vials and stirred for 5 minutes using a magnetic stirrer followed by drop wise addition of 2 ml of water. The solution was transferred in to plastic moulds and placed in a dry ice container for 2 hours. The samples were in specimen of 2 x 2 x 1.5 cm. They were stored in vacuum until use. A pilot study was intended to test the effect of the ceramic (bovine hydroxyapatite) on osteoblast function. From the results of the pilot study we designed the main study. The main study was

designed to study the effect of increase in the ceramic concentration on bone marrow stem cell differentiation.

The plastic moulds were lyophilized for about 24-48 hours to ensure complete evaporation of the solvent. Similarly we initially weighed the polymer (1g) and ceramic (1g) and mixed the two powders and prepared PLGA-B-HA composites (1:1, 1:2 and 1:3) in a similar manner as described above. The samples were cut using a razor blade in the dimensions of 12 x 11 x 2 mm**.** Prior freezing in liquid nitrogen was not done for this study as it was understood that this mechanism could disrupt the morphological structure of the composite.

2.2 Cell isolation, seeding and culture

Fig. 1 Represents the isolation procedure of rat marrow stem cells.

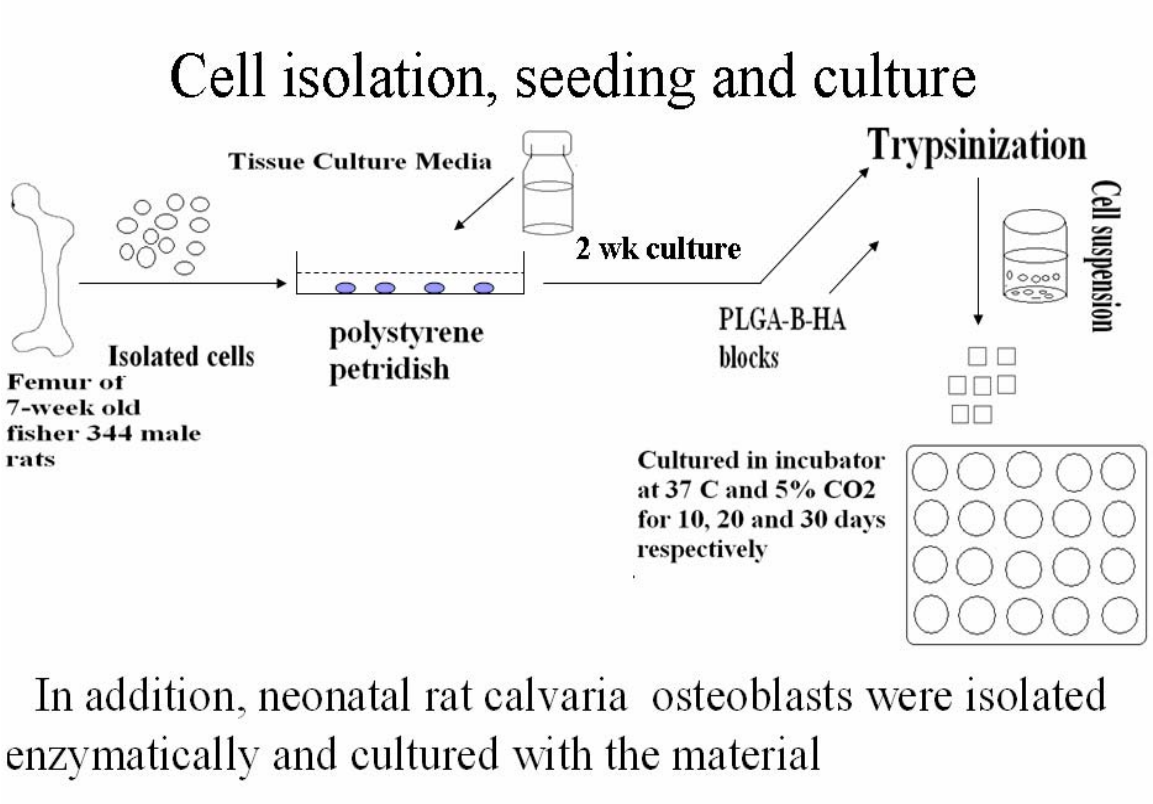

Figure 1. The isolation technique of bone marrow stem cells from the femora of 7-week old Fisher 344 male rats.

The two different types of cells that are used for this experiment were the neonatal rat calvarial osteoblasts (NRCO) and bone marrow stem cells (BMSC's). Neonatal rat calvarial osteoblasts were isolated using a collagenase digestion technique. Two T-25 cm^2 flasks containing 50 ml of PBS 50 and 34 µL of antibiotic respectively are taken. Neonatal rat calvarial cells were isolated and cultured in the flask containing 50 µL of antibiotic solution. The flask cap is then tightened and placed and in an ice box. Calvaria from the brain tissue are cleaned in a sterile petridish and are made free from the extra

tissue. The tissue is then transferred into 50 ml PBS solution prepared earlier. The PBS is then pipetted out from the flask without disturbing the cleaned calvarial tissue. 5 ml of collagenase-2 is added and is followed by the addition of 1 ml of trypsin. The flask cap is tightened and stirred for 20 minutes and the solution is transferred in centrifuge tubes. The tubes were centrifuged 400g for 10 minutes. The supernatant containing the enzyme is transferred to the flask containing calvarial tissue and the cell pellet from the first extraction is discarded. The second extraction was discarded and cells from subsequent extractions were used for the experiment. For the third extraction the supernatant was transferred in a tube and centrifuged at 400g for 10 minutes. The supernatant was removed and 2 ml of media containing 10% Fetal Bovine Serum (FBS), 0.06% fungizone, 0.1% antibiotic (penicillin) were added. The cell pellets are broken by repeated pipetting and are further cultured in T-75 cm^2 flasks in the incubator. The media was changed after every 2-3 days. The cells were maintained in T-75 cm^2 flasks. α Minimally Essential Medium (αMEM) (Invitrogen Technologies, Grand Island, NY) containing 10% Fetal Bovine Serum (FBS), 0.06% fungizone, 0.1% antibiotic (penicillin) was used *in vitro* cell culture experiments.

The samples were initially sterilized in 70 % ethanol for 2 ½ hours. The cells were seeded on to the scaffold giving a concentration of 50,000 cells/scaffold. The samples (positive and negative control) were cultured in a 24-well plate immersed in 2 ml of media. The other well plate consisted of pure HA (Interpore 200) seeded with NRCO immersed in tissue culture medium. The cells were cultured for a period of 2 weeks and morphology was analyzed using SEM/EDX. In the other study bone marrow stem cells were isolated from the femora of 7-week old 344 Fisher male rats. Following euthanasia by CO_2

inhalation, the femurs were aseptically excised, cleaned of soft tissue, and washed in αMinimally Essential Medium (αMEM) (Invitrogen Technologies, Grand Island, NY) containing 10% fetal bovine serum (FBS), 0.06% fungizone, 0.1% antibiotic (penicillin) and 3mM Na β-glycerophosphate (Sigma). Essential Medium (αMEM) containing the above mentioned composition along with 50 μg/mL L-Ascorbic acid (Sigma) and 10^{-8} M dexamethasone (Sigma) was used *in vitro* cell culture experiments. The metaphyseal ends were then cut off and the marrow was flushed from the midshaft with 5-6 ml of media using a syringe equipped with an 18 ½ G needle and collected in a sterile petridish. Cell clumps were broken by repeatedly pipetting the cell suspension using 20 ½ G, 22 ½ G and 23 G needles. The cells then were centrifuged at 500g for 5 min. The resulting cell pellets were resuspended in 13 mL of media and plated in T-75 flasks (cells from two femurs per flask). After 24 hours, hematopoietic cells and other unattached cells were removed from the flasks. Once 70% confluency was reached the cells were enzymatically lifted using 5-6 mL trypsin per flask. The cells were concentrated by centrifugation at 500g for 5 min and resuspended in 2 mL media. Cells were counted with a hematocytometer in complete media [consisting of α- MEM supplemented with 10% FBS, 3mM Na β-glycerophosphate, 50 μg/mL L-ascorbic acid (Sigma)] containing 10^{-8} M dexamethasone (Sigma) to promote the differentiation of bone marrow stromal cells to osteoblastic phenotypes. Aliquots of cell suspensions were seeded onto the top of prewetted foams placed in the wells of 24 well plates, resulting in seeding densities equivalent to 250,000 cells/scaffold. The 24-well plate was left undisturbed in the sterile hood for 6 min to allow the cells to attach after which an additional 2 ml of complete media was added. Media was replaced after every 2-3 days. The control was used as a

comparison for the alkaline phosphatase activity and for a qualitative assessment of the mineralization.

2.3 Material Characterization

2.3.1 Fourier transform infrared spectroscopy Analysis (FTIR)

1:1, 1:2 and 1:3 PLGA-B-HA composites were analyzed using Fourier Transform Infrared Spectroscopy. The data was collected using the Nexus 670 (Thermo Nicolet Inc) using KBr as the background. The samples are placed within the sample holder and the characteristic peaks are analyzed using the diffuse reflectance method.

2.3.2 Electron microscopy

PLGA-B-HA composites and pure HA discs seeded with and without cells were analyzed using Scanning Electron Microscopy. Samples with cells are repeatedly washed with PBS in a 24 well plate to remove the unattached substrates on to the surface. The samples are placed in a fixative (10% formaldehyde or glutaraldehyde) and stored in the refrigerator. Further they are dehydrated in ethanol series (50%, 60%, 70%, 80%, 90%, 95% and 100%). The samples were dehydrated in 50-70% for at least 5 minutes and 10 minutes for the rest. The samples are then rinsed in Fluorotrichloromethane (Fereon) and coated with gold palladium prior to SEM analysis. The SEM is a Hitachi Model S-3200-N with a resolution of 3.5 nm. It is equipped with a Noran Energy Dispersive Spectroscopy {EDS} system, which permits elemental analysis down to Boron. The Sputter Coater is a model SC - 400 Emscope. The target material is AuPd. We sputter with argon at a pressure of 0.07 Torr for a period of one minute.

2.3.3 Mechanical testing

The compressive mechanical properties of the composites were tested with a custom built Compression testing machine (Center for Biomedical Engineering, University of Kentucky, Lexington, KY). The displacement rate was set at 0.5 mm/min. At least 3 specimens were tested for each sample. The results were expressed as means ± standard deviations.

2.3.4 Surface roughness characterization

2.3.4.1 Qualitative analysis of surface roughness

The ZYGO New View 5000 scanning white light interference microscope and scanning electron microscopy were used to characterize surface roughness**.** A qualitative analysis of the roughness was performed by scanning electron microscopy (SEM). The SEM is a Hitachi Model S-3200-N with a resolution of 3.5 nm.

2.3.4.2 Quantitative analysis of surface roughness

Quantitative analysis of the roughness was performed by the ZYGO New View 5000 scanning white light interference microscope (ZYGO Corporation, Middlefield, CT, U.S.A). The New View is a precision microscope which uses scanning white light interferometry to generate quantitative three dimensional images. Zygo's MetroPro ™ software provides an interactive window display, surface images, plots and data. PLGA-B-HA composites 1:1, 1:2 and 1:3 respectively were coated with aluminum. The PLGA-B-HA composites were coated with aluminum using a sputtering machine (AJA International, Kurt Lesker Inc.) with a coating time and thickness 230 seconds and 20 nm respectively at 3 millitorr pressure. 10 readings representing approximately an area of 1 x

200 µm were performed randomly corresponding to the different areas on the samples. 2.5X Mich (10X) were used with image zoom to measure the samples. Surface roughness values were expressed as average roughness (Ra), root mean square roughness (Rrms) and peak value (Rp). Rrms values give a good general description of the structure of the actual surface. R_a is the arithmetic mean of the departures of the roughness profile from the mean area.

$$R_a = \frac{1}{n}\sum_{i=1}^{n}|Z_i|, \qquad (1)$$

Where Zi is the i^{th} dot of the distance to the center line, *n* is the total number of sampling dots, and Rrms, is the root mean-square deviation from the profile mean over the sampling area, corresponding to Ra [54]:

$$R_{rms} = \sqrt{\frac{1}{n}\sum_{i=1}^{n}[Z_i]^2} \qquad (2)$$

PV (Peak-to valley) is the distance between the highest and the lowest points within the sample [55-56]. In the current study Ra, Rrms and Rp values were calculated directly by New View software.

2.4 Bioactivity Evaluation

2.4.1 Alkaline phosphatase assay

Production of alkaline phosphatase (ALPase) was measured spectroscopically. Osteoblast-seeded foams and 2-D osteoblast cultures at the end of 10, 20 and 30 days were washed with PBS and lysed using 1% Triton-X 100 (Aldrich Chemical Company Incorporation) and the osteoblasts of the 2-D control cultures were scraped from the well bottoms, using disposable cell scrapers, into 500 µL 1 % Triton-X 100. The sets were

sonicated (FS 30, Fisher scientific incorporation) at 1300 rpm for 3min. The supernatant was removed and transferred in new sets of micro tubes. The scaffolds were resuspended in 500 µL 1 % Triton-X 100 and the same procedure was followed. The two supernatants were combined and the resultant was used to measure the AP assay. The production of p-nitrophenol in the presence of phosphatase substrate (Sigma, Inc.) was measured by monitoring light absorbance by the solution at 410 nm at 5min increments. The slope of the absorbance versus time plot was used to calculate the ALpase activity.

2.4.2 Osteocalcin

Bone marrow stem cells extracted from 7-week old Fisher 344 male rats were grown to confluence (day 30) in culture medium. The medium was collected and stored at -20^{o} C until assay for osteocalcin. Osteocalcin concentration for 1:1, 1:2, 1:3 and control samples was measured at the end of 14, 21 and 28 days respectively in tissue culture medium. Determination of osteocalcin was performed in duplicate with an ELISA assay (Biomedical Technologies Incorporation, MA, U.S.A); the detection range of the kit was 0.3-20 ng/ml**.**

2.5 Corrosion studies in tissue culture medium

The degradation rates were measured for 1:1, 1:2 and 1:3 PLGA-B-HA composites at the end of 7, 14, 21 and 28 days by Optima 2000 DV used for ICP analysis. Four replicates of each composition i.e. 64 samples in total were analyzed. pH measurements were taken at the end of 28 days following immersion. The samples were diluted in 1:4 dilutions using deionized water. The washing solution used in the experiment was 4% HNO_3. The samples were analyzed for Ca and P concentrations respectively.

2.6 Statistical analysis

Two-way ANNOVA (assuming unequal variances) was performed to determine the statistical significance ($p < 0.05$) in the mean value of measured parameters between the different experimental groups.

CHAPTER THREE

RESULTS

3.1 Pilot study

3.1.1 Characterization of the material

3.1.1.1 Surface morphology of PLGA-B-HA composite

SEM analysis indicated the external morphology of the PLGA-B-HA composite is highly porous with the pore size varying from 30-1000 microns (Fig. 2). The arrows point to the different pore sizes.

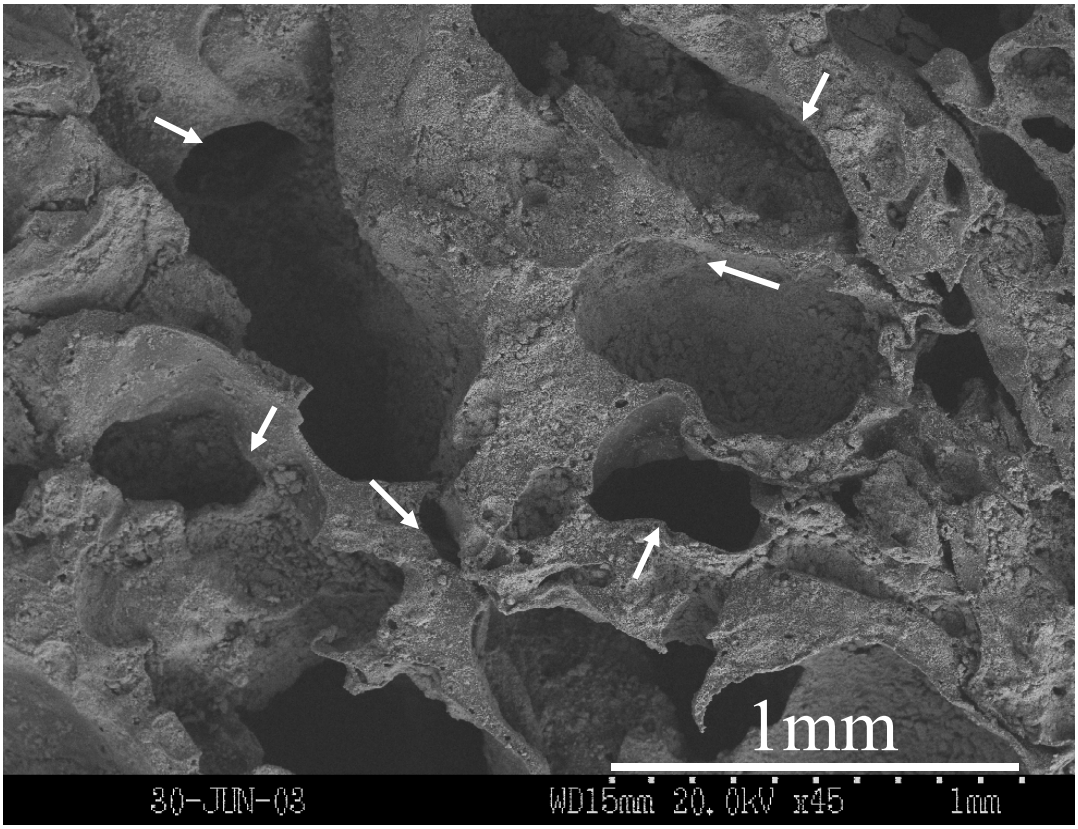

Figure 2. External morphology of the PLGA-B-HA composite. The SEM analysis showed that the composite is highly porous with the pore size varying from 30-1000 microns. The arrows point to pores of various sizes.

Higher magnification indicated that the inner walls of the composite were also porous with the pore size varying from 20-1000 nm (Fig. 3). This indicates that the composite has an open or an interconnected morphology. Also, we could observe a uniform distribution of ceramic particles within the polymeric phase as indicated by the arrows.

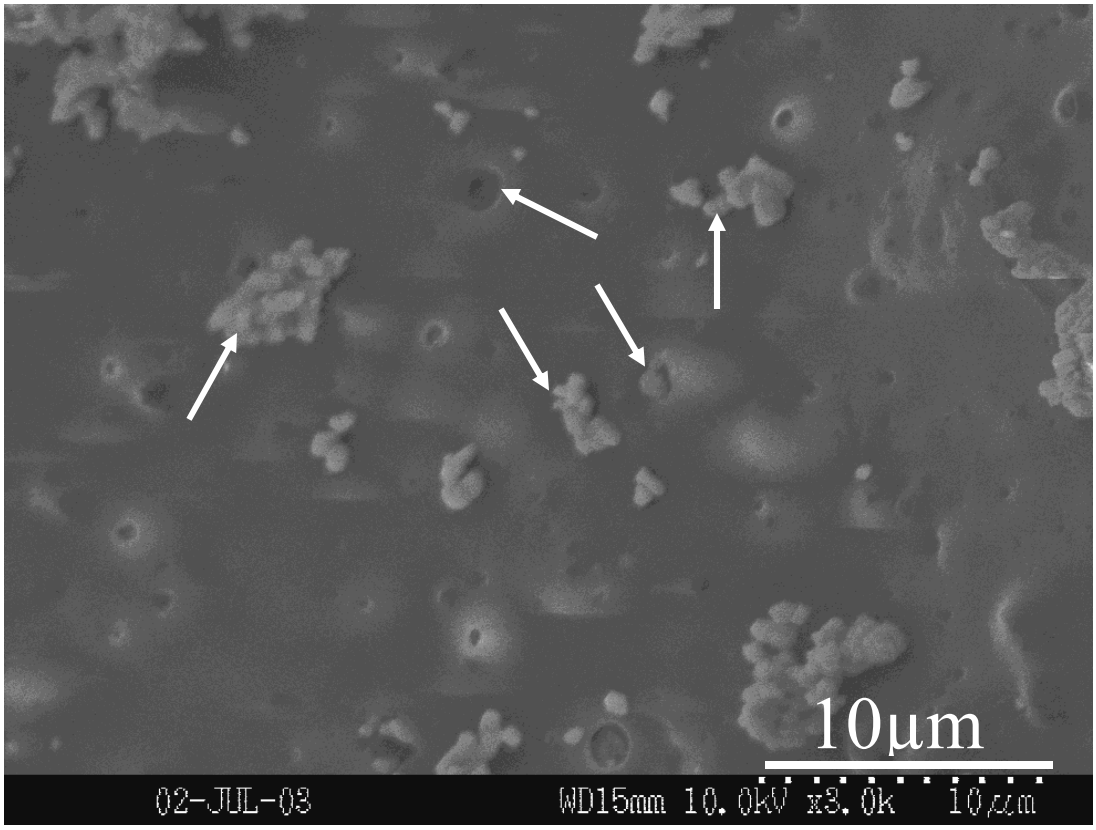

Figure 3. Higher magnification of the wall of a pore as indicated in Figure 2. The inner surface is also porous with the pore size varying from 20-1000 nm. The arrows indicate the homogenous distribution of the ceramic particles and this is the surface where the cells are getting attached to. From the figure we can draw a conclusion that the scaffold acquired an open porous structure with an interconnected pore network.

3.1.1.2 SEM analysis of the composite material

SEM analysis (Fig.4) shows the ceramic particles (arrows) were covering the surface of the surface of the pores.

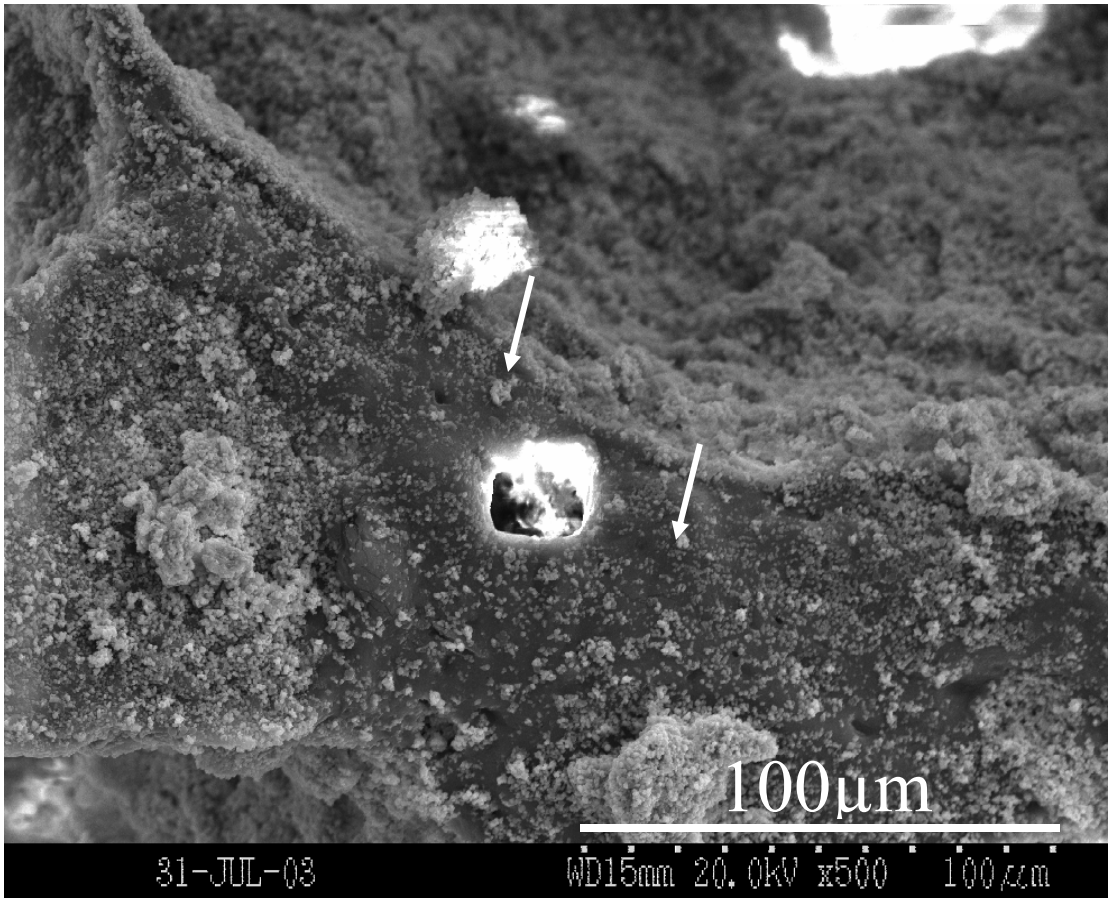

Figure 4. SEM analysis of the PLGA-B-HA composite without cells. The figure indicates the uniform distribution of the ceramic particles on the polymeric matrix. The arrows point to B-HA particles.

EDX analysis shows a Ca/P ratio of 1.67 (Fig.5). This ratio confirms the presence of the HA ceramic incorporated in the polymer.

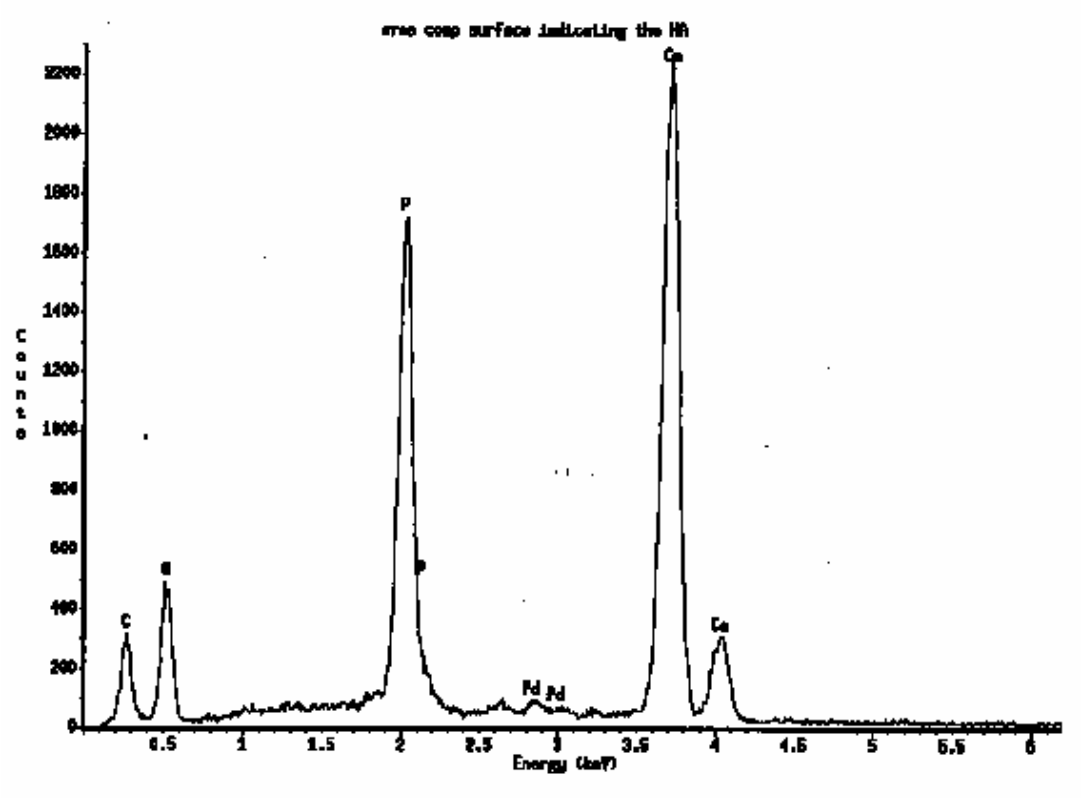

Element	k-ratio (calc.)	ZAF	Atom %	Element Wt %	Wt % Err. (1-Sigma)	No. of Cations
C -K	0.0489	3.914	30.32	19.14	+/- 0.46	14.726
O -K	0.0562	7.393	49.41	41.54	+/- 0.83	---
P -K	0.0903	1.274	7.07	11.51	+/- 0.14	3.435
Ca-K	0.2486	1.119	13.20	27.81	+/- 0.24	6.413
Total			100.00	100.00		24.573

Figure 5. EDX analysis of PLGA-B-HA composite without cells. The Ca/P ratio in this case is equal to be 1.67. The EDX analysis indicated the high Ca and P content indicating that these are the ceramic particles.

3.1.2 Cell adhesion and Morphology

3.1.2.1 Evaluation of pure HA discs (Interpore 200) seeded with neonatal rat calvarial osteoblasts

SEM analysis after 2 weeks in culture showed neonatal rat calvarial osteoblasts attached to the surface of the ceramic and formed unmineralized cell layer. Fig. 6 is an SEM analysis of the cell layer demonstrating that the surface of the cell is smooth and void of any calcified nodules. Beneath the non mineralized cell layer '**C',** a dense collagenous matrix is observed.

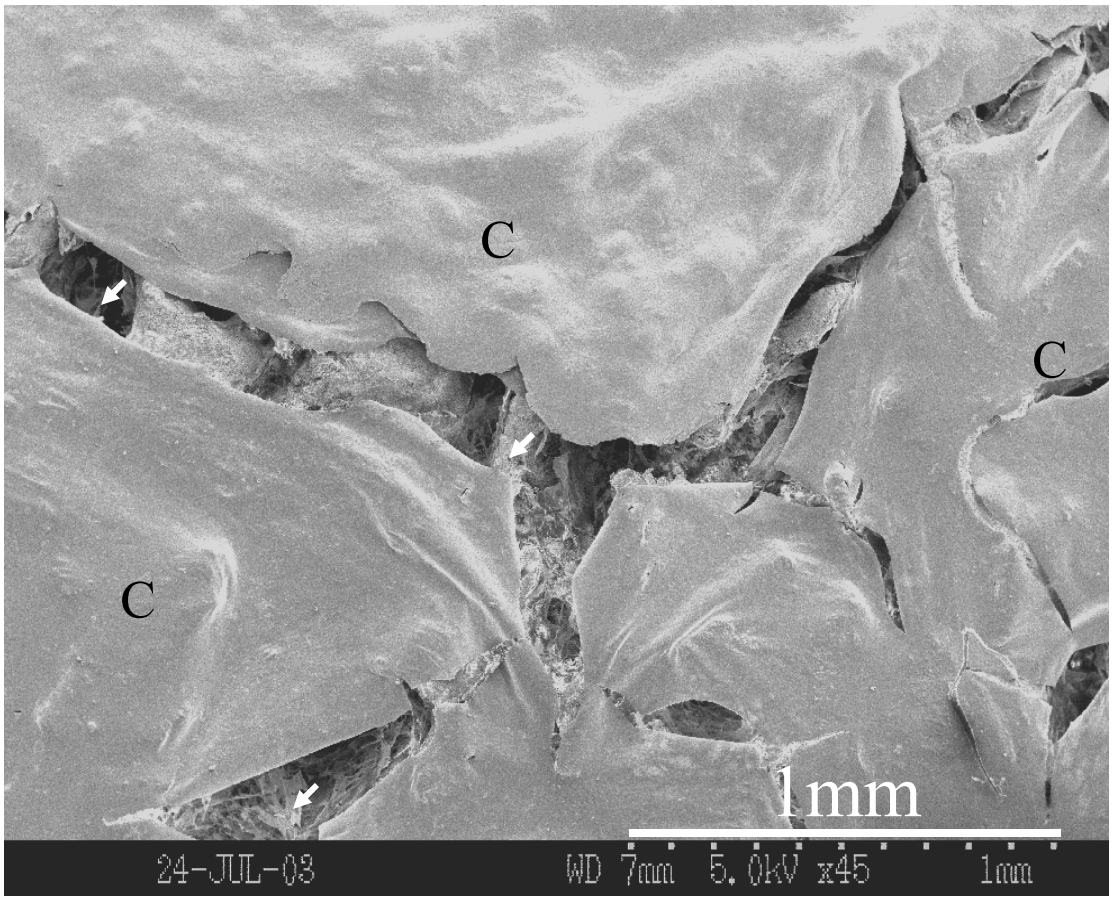

Figure 6. SEM image of the hydroxyapatite ceramic surface cultured with neonatal rat calvarial cells for 2 weeks. The figure indicated the formation of a cell layer (c) with

unmineralized extracellular matrix. It is worthy to note the absence of calcified nodules on the cell surface. The arrows point out to the collagenous matrix beneath the cell layer.

At some places a network of collagen fibers could be observed (Fig. 7) whereas at some places we could observe the fusion of the collagen fibers to form a dense layer of ECM. An important thing to be noted here is the absence of calcified nodules or mineralized matrix.

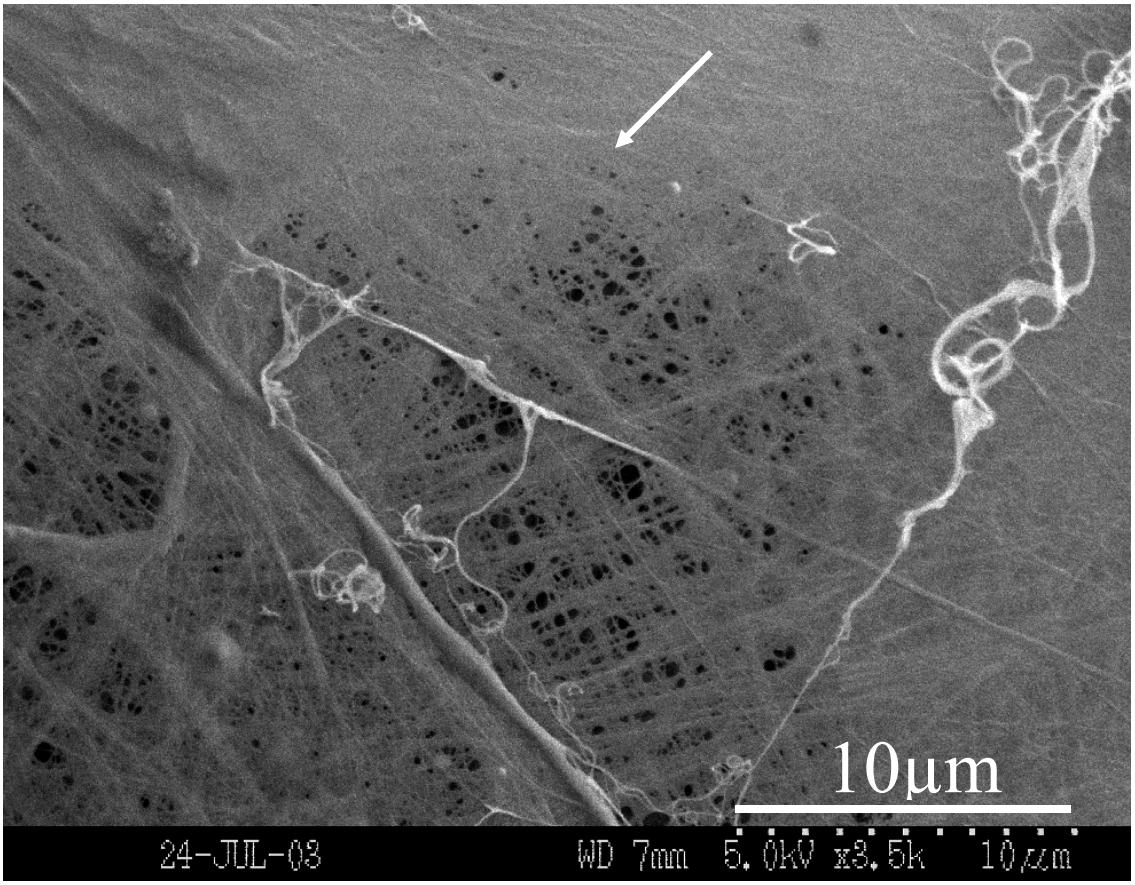

Figure 7. Neonatal rat calvarial cells cultured on to the surface of HA ceramic for 2 weeks. In some areas non mineralized collagen fibers were seen covering the surface and forming a network. Collagenous fibers network fused together in some areas to make a

continuous sheet of ECM on the ceramic surface. It is worth to note the complete absence of calcified nodules.

3.1.2.2 Evaluation of PLGA-B-HA composites seeded with neonatal rat calvarial osteoblasts

SEM analysis indicated (Fig.8) that neonatal rat calvarial osteoblasts attached to PLGA-B-HA composites formed mineralized extra cellular matrix and calcified nodules after 2 weeks in culture.

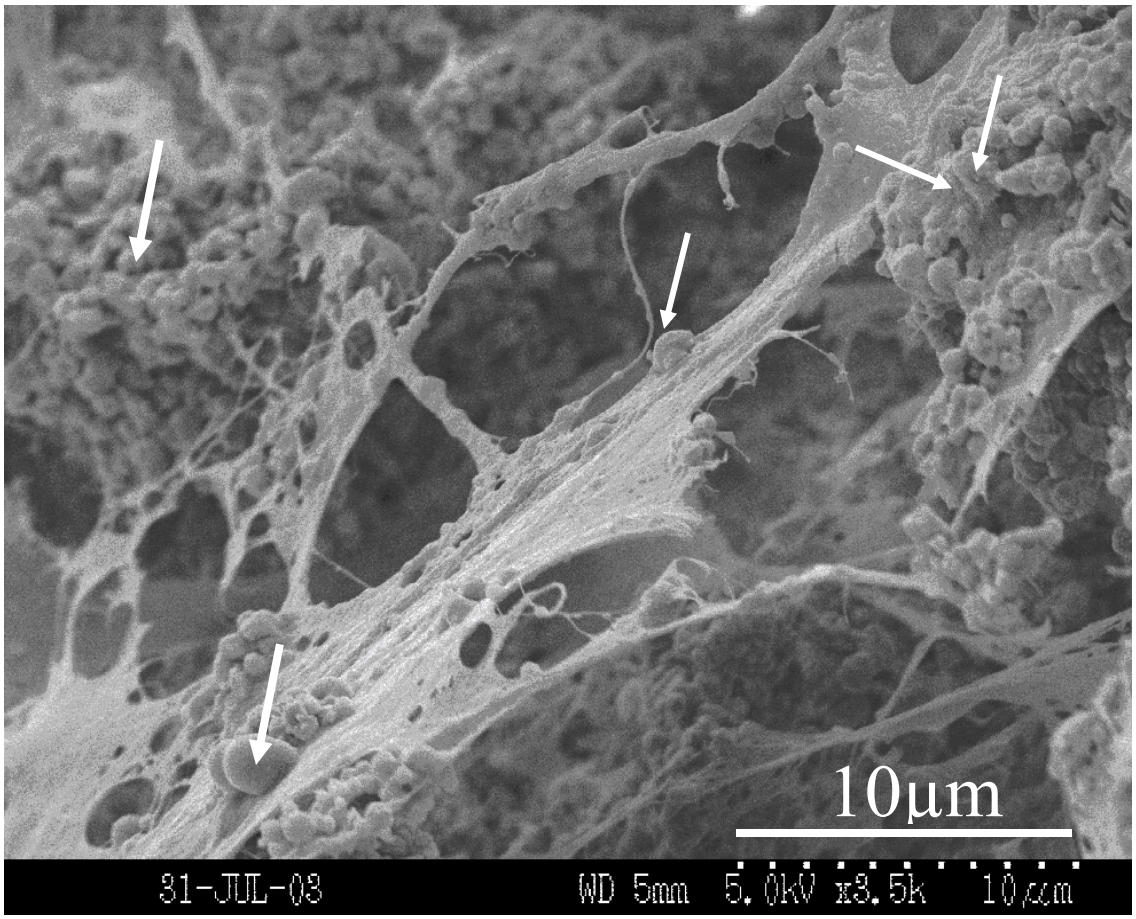

Figure 8. Neonatal rat calvarial cells cultured on to PLGA-B-HA composites for 2 weeks. In contrast we could observe a dense mineralized, extracellular matrix formation or calcified nodules on to the surface of the collagenous matrix. Calcified nodules are

seen to be deposited on the surface of the collagen fibers as well as the bone like tissue. Also at some areas we could observe interaction between the calcified nodules and the collagenous fibers as indicated by the arrows. Mineralized extracellular matrix filled the pores and covered the surface of the template.

Fig. 9 represents EDX analysis of the calcified nodules produced by the neonatal rat calvarial cells cultured on PLGA-B-HA composites for 2 weeks. The Ca/P ratio as indicated in the figure is equal to 1.66.

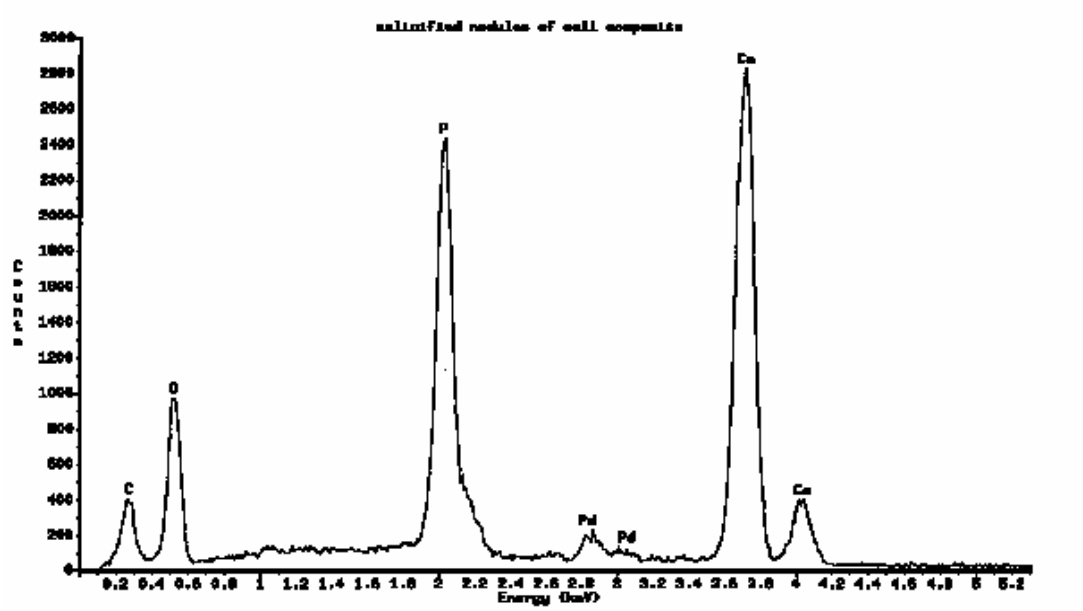

Element	k-ratio (calc.)	ZAF	Atom %	Element Wt %	Wt % Err. (1-Sigma)	No. of Cations
C -K	0.0442	3.837	26.14	16.95	+/- 0.39	11.078
O -K	0.0759	6.443	56.64	48.91	+/- 0.69	---
P -K	0.0820	1.290	6.33	10.59	+/- 0.12	2.683
Ca-K	0.2097	1.123	10.89	23.55	+/- 0.18	4.613
Total			100.00	100.00		18.375

Figure 9. EDX analysis of the calcified nodules produced by the cells on the PLGA-B-HA composite surface. The EDX analysis of the calcified nodules showed a Ca/P ratio of 1.66.

Fig. 10 indicates the higher magnification of the calcified nodules. The arrows indicate the immediate interaction between the calcified nodules and the collagen fibers. The calcified nodules varied in the size range from 50-500 nm. Large numbers of calcified nodules were seen covering the extracellular matrix (collagen fibers) in certain areas on the composite surface.

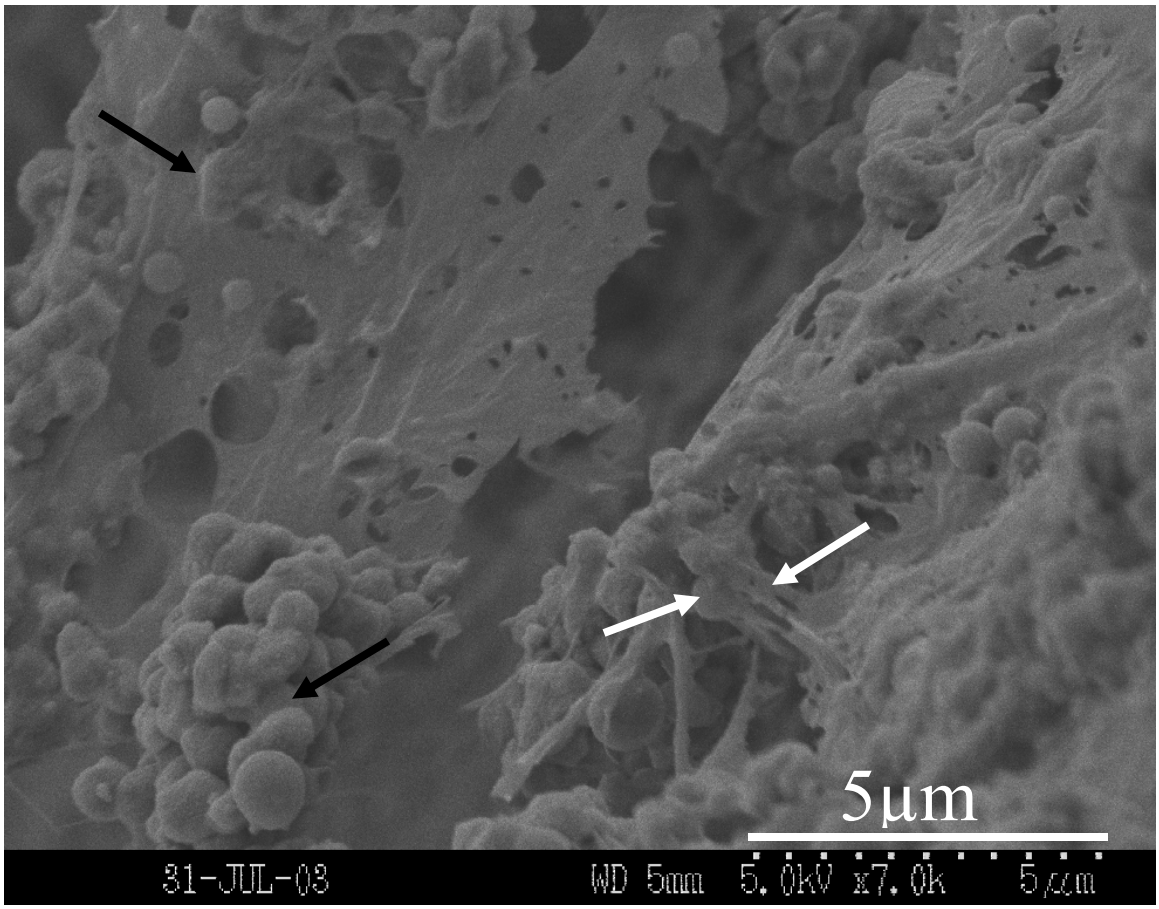

HA

Figure 10. Higher magnification indicating the formation of a mineralized (ECM) layer secreted by the cells seeded on to the PLGA-B-HA composite. In some places we can observe accumulation of calcified nodules and the size of the nodules varied from 50-500 nm as indicated by the black arrows. Calcified nodules are seen to be deposited on the surface of the collagen fibers as well as the bone like tissue. The white arrows point to the

intimate interaction between the calcified nodules and the collagen fibers produced by cells.

Also, we could observe the connection of pores via collagen fibers. The EDX analysis of the calcified nodules confirms the secretion of inorganic bone mineral (hydroxyapatite) by the cells with a Ca/P ratio equal to 1.67 (Fig.11).

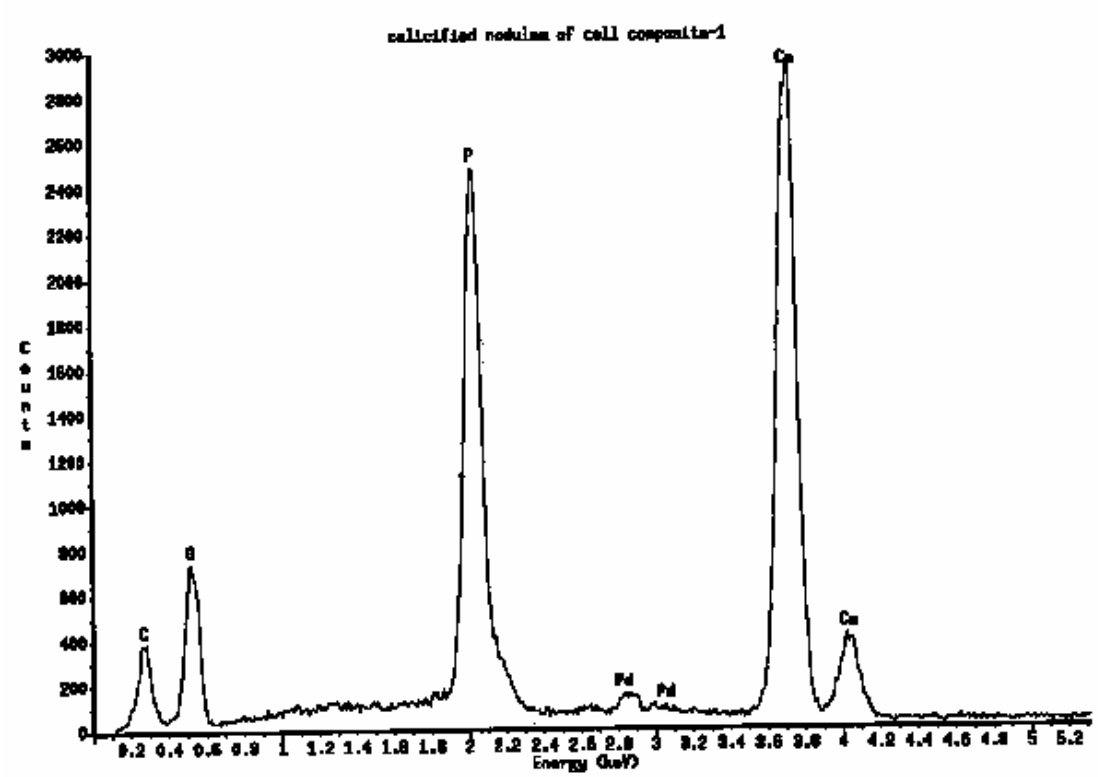

Element	k-ratio (calc.)	ZAF	Atom %	Element Wt %	Wt % Err. (1-Sigma)	No. of Cations
C -K	0.0455	4.009	28.64	18.25	+/- 0.40	13.207
O -K	0.0631	6.998	52.05	44.19	+/- 0.70	---
P -K	0.0927	1.278	7.21	11.85	+/- 0.13	3.324
Ca-K	0.2292	1.122	12.09	25.71	+/- 0.19	5.575
Total			100.00	100.00		22.106

Figure 11. EDX analysis of the interaction between the calcified nodules and the collagen fibers secreted by the cells. EDX analyses indicated that the calcified nodules are composed of mineralized hydroxyapatite with a Ca/P ratio equal to 1.67.

A dense layer of calcified matrix could be observed within a crack in the pore wall of the material (Fig. 12). Beneath the crack we could observe spherical shaped particles as indicated by the white arrow. A significant difference could be observed in the morphology of the particles secreted by the cells and the ceramic particles used in the study. The ceramic particles are irregular shaped whereas the calcium phosphate particles secreted by the cells are spherical in shape.

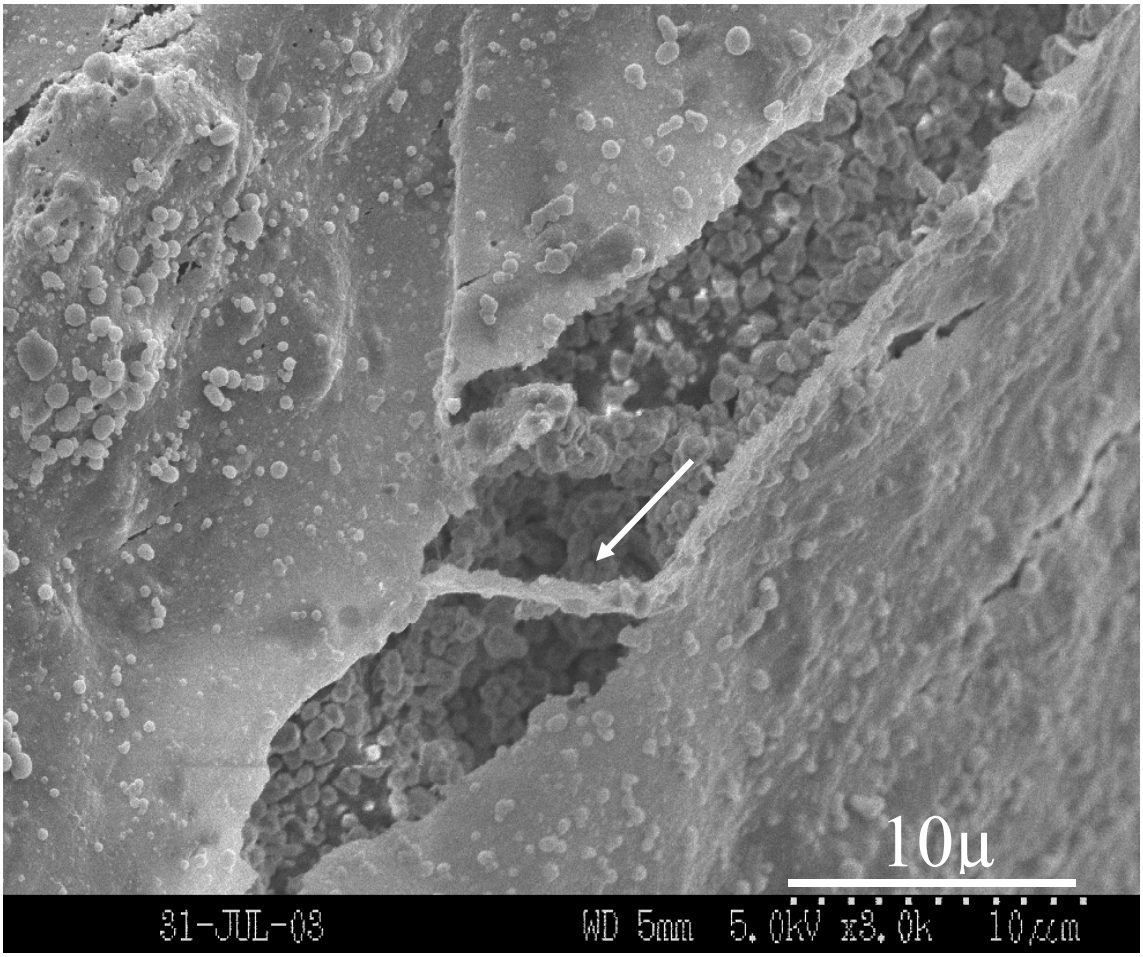

Figure 12. Indicating an area under the crack in the cell layer within the pore wall of PLGA-B-HA composite seeded with cells. The figure describes the formation of a layer of tissue within the area under a crack.

Figure 13 indicates the EDX analysis of the area under the crack within the cell layer in a pore. The EDX analysis indicates the Ca:P ratio of the cell layer to be 1.66 closer to the inorganic component of bone.

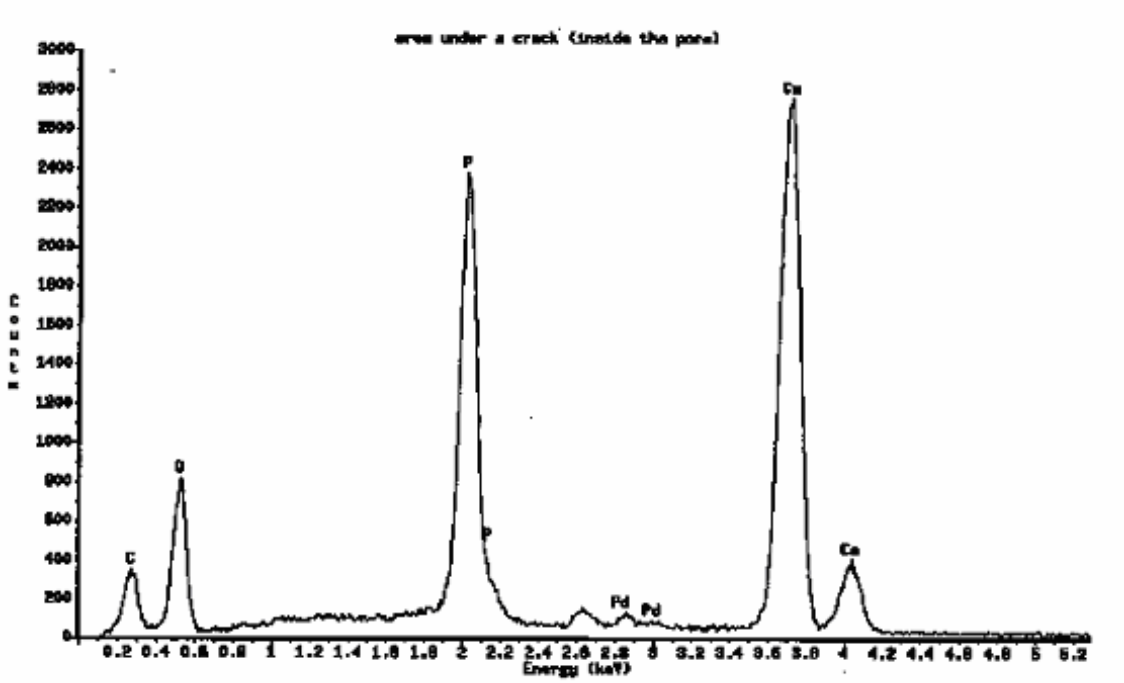

Element	k-ratio (calc.)	ZAF	Atom %	Element Wt %	Wt % Err. (1-Sigma)	No. of Cations
C -K	0.0420	4.010	26.49	16.86	+/- 0.40	11.673
O -K	0.0681	6.776	54.47	46.16	+/- 0.71	---
P -K	0.0913	1.282	7.14	11.71	+/- 0.13	3.146
Ca-K	0.2252	1.122	11.90	25.27	+/- 0.20	5.244
Total			100.00	100.00		20.063

Figure 13. EDX analysis of an area under a crack in the cell layer within the pore wall. The EDX analysis indicates the high content of the Ca and P which indicates the cellular activity. The Ca/P ratio in this case was equal to be 1.66 that indicates that the ratio is close to the natural hydroxyapatite material**.**

3.2 Main study

3.2.1 Effect of the chemical composition on the morphology of 1:1, 1:2 and 1:3 PLGA-B-HA composites

3.2.1.1 Qualitative analysis of surface roughness using SEM

Comparing the morphologies of 1:1, 1:2 and 1:3 we observe that the samples are highly porous with the porosity varying from 40-1000 μ (Fig. 14, Fig. 15 and Fig. 16). 1:1 PLGA B-HA composite indicated the presence of comparatively thinner pore wall with an average thickness of 85 μ. The pore walls are indicated by the black arrows (Fig. 14).

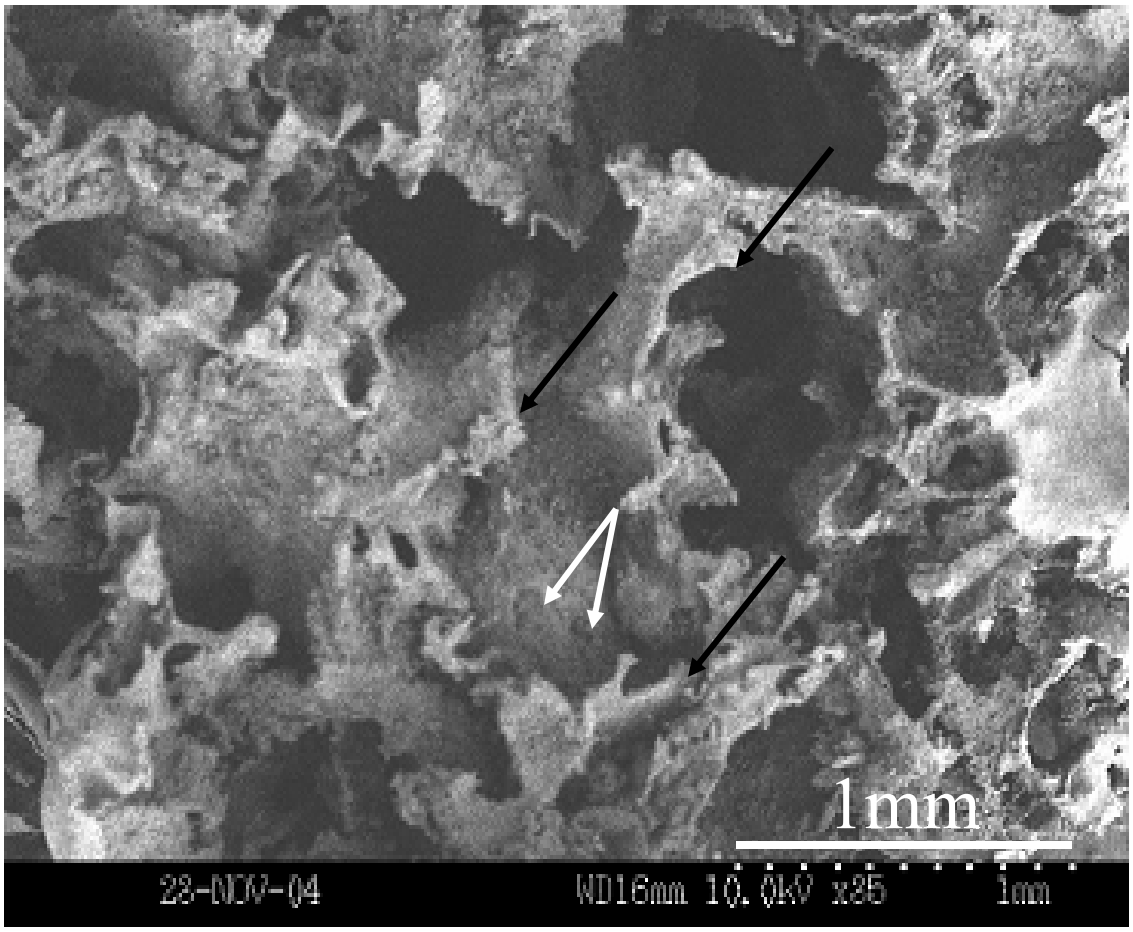

Figure 14. The figure shows the external morphology of 1:1 PLGA-B-HA composite. The figure indicates the composite is highly porous with the pore size varying from 40 -

1000µ. The inner surface of the composite is also highly porous with the pore size varying from 10-90 µ as indicated by the white arrows. The pore walls are significantly ($p < 0.05$) thinner and are indicated by the black arrows. The average pore wall thickness of the 1:1 PLGA-B-HA composite is equal to 85µ.

Smaller pores as indicated by the red arrows within the pores with a pore size range varying from 10-90 μ could be observed. The pore walls of 1:2 PLGA-B-HA composite are thicker as compared to 1:1 PLGA-B-HA composites and are indicated by black arrows (Fig. 15). The pore size varied in the range 60-1000 μ.Also, in 1:2 PLGA-B-HA composite, smaller pores as indicated by the red arrows could be observed within the pore walls of the larger pores. The smaller pores varied in the size range from 10-40 μ. The average pore wall thickness of 1:2 PLGA-B-HA composite equals 130 μ

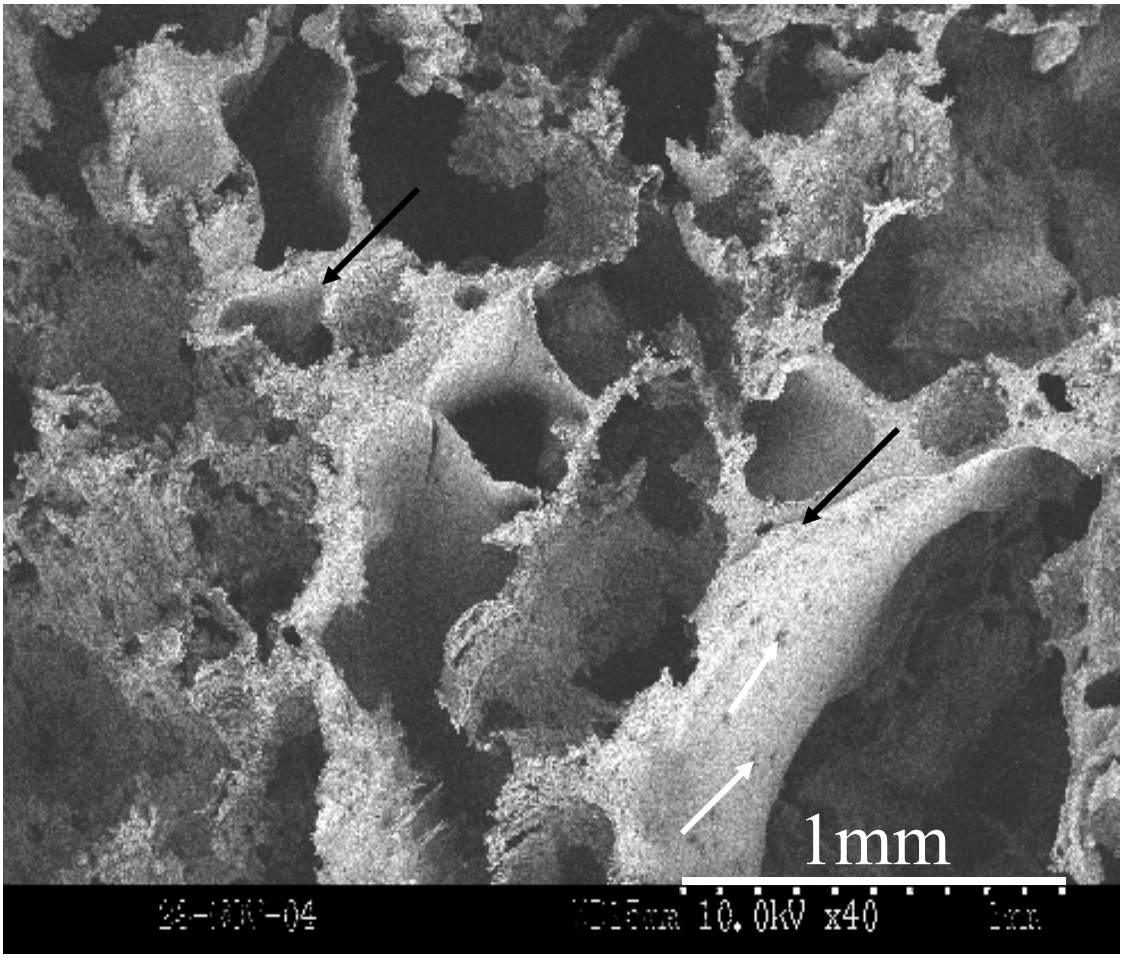

Figure 15. The figure shows the external morphology of 1:2 PLGA-B-HA composite. The figure indicates that the composite is highly porous with the pore size varying from 60 - 1000μ. The inner surface of the composite is also highly porous with the pore size

varying from 10-40 μ as indicated by the white arrows. The pore walls are significantly ($p < 0.05$) thicker as compared to 1:1 PLGA-B-HA composites and are indicated by the black arrows. The average pore wall thickness of the 1:2 PLGA-B-HA composite equals 130μ.

Thicker pore walls could be observed in 1:3 as compared to 1:1 and 1:2 PLGA-B-HA composites and are indicated by arrows (Fig. 16). The pore size varied in the range 30-1000 µ. The average pore wall thickness of the 1:3 PLGA-B-HA composite was equal to 182 µ. Also, here absence of smaller pores within the pore walls could be observed. The composites appear to be rougher as compared to 1:1 and 1:2 PLGA-B-HA composites. 1:2 PLGA-B-HA composites appear to be rougher than 1:1 PLGA-B-HA composites.

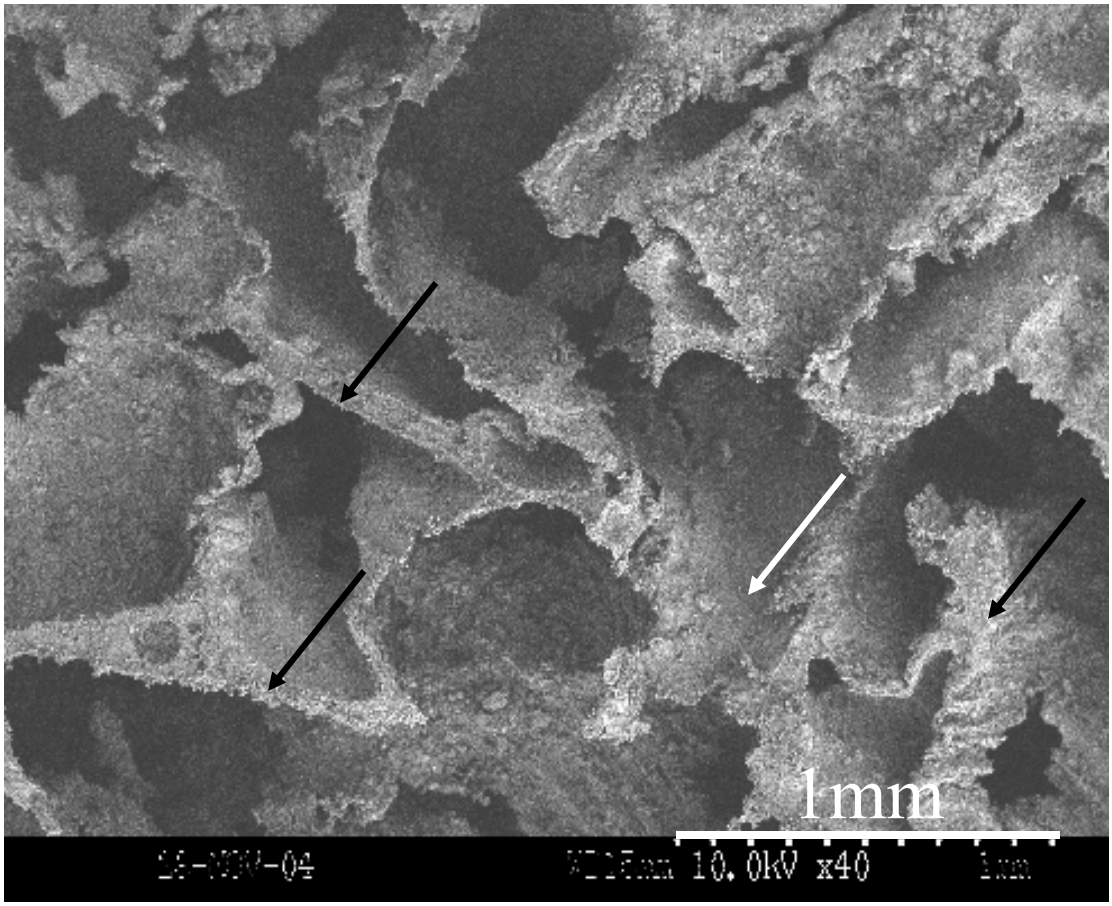

Figure 16. The figure shows the external morphology of 1:3 PLGA-B-HA composite. The figure indicates the composite is highly porous with the pore size varying from 30 - 1000µ. Here no inner pores could be observed as indicated by the white arrow. The pore walls are significantly ($p < 0.05$) thicker as compared to 1:1 and 1:2 PLGA-B-HA

composites and are indicated by the black arrows. The average pore wall thickness of the1:3 PLGA-B-HA composite equals 182µ.

Table1. Indicates the average pore wall thickness of 1:1, 1:2 and 1:3 PLGA-B-HA composites. The results indicate a significant increase in the pore wall thickness in the order of 1:3 > 1:2 > 1:1 could be observed.

SAMPLES	PORE WALL THICKNESS	p-VALUES 1:1 & 1:2	p-VALUES 1:1 &1:3	p-VALUES 1:2 & 1:3
1:1	85±29.155			
1:2	130±49.22	0.025	0.00032	0.04
1:3	182±57			

Table 1. Indicates average pore wall thickness of 1:1, 1:2 and 1:3 PLGA-B-HA composites. The table also provides a statistical comparison of the average pore wall thickness of the 1:1, 1:2 and 1:3 PLGA-B-HA composites.

3.2.1.2 Quantitative analysis of surface roughness using the "New View 5000"

Quantitative analysis of surface roughness was done using the "New View 5000" scanning white light interference microscope.

Figure17. Represents the surface of 1:1 PLGA-B-HA composite. The arrow indicates the area to be scanned.

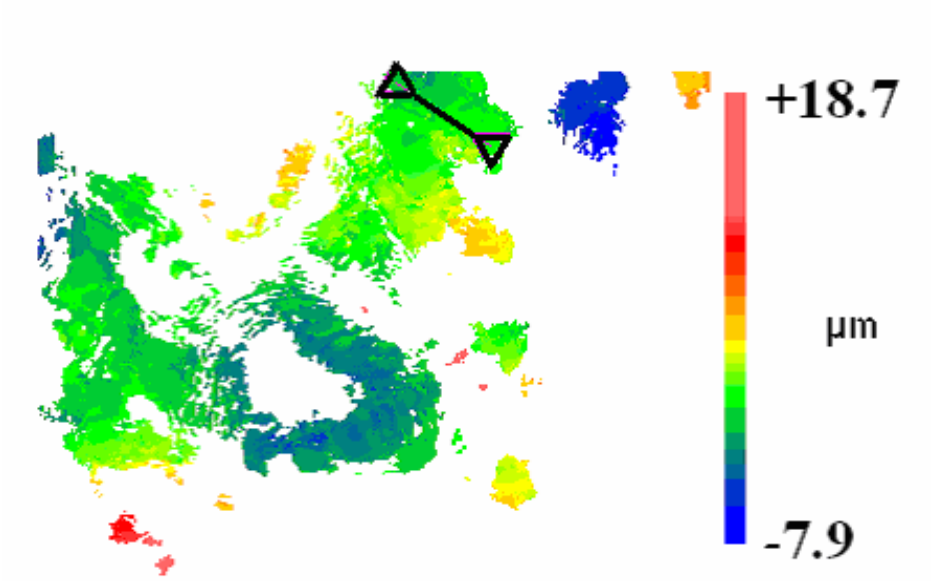

Figure 17. The color contour is represented by the micron scale and varies from -7.9 to + 18.7 µm. The positive value corresponds to the peaks whereas the negative value corresponds to the valleys. The peaks are indicated by the green, yellow and red areas. The valleys are indicated by the blue areas.

Fig. 18, Fig.21 and Fig. 24 describes the oblique plots of randomly selected areas on 1:1, 1:2 and 1:3 PLGA-B-HA composites respectively. Fig.18. indicates the presence of peaks indicated by the green lines. The scanning depth of the selected area varied from -1.46 to +1.8 µm. Few peaks with increased heights up to 1.8 µm could be seen on the surface and are indicated by red lines. The valleys are indicated by the blue lines.

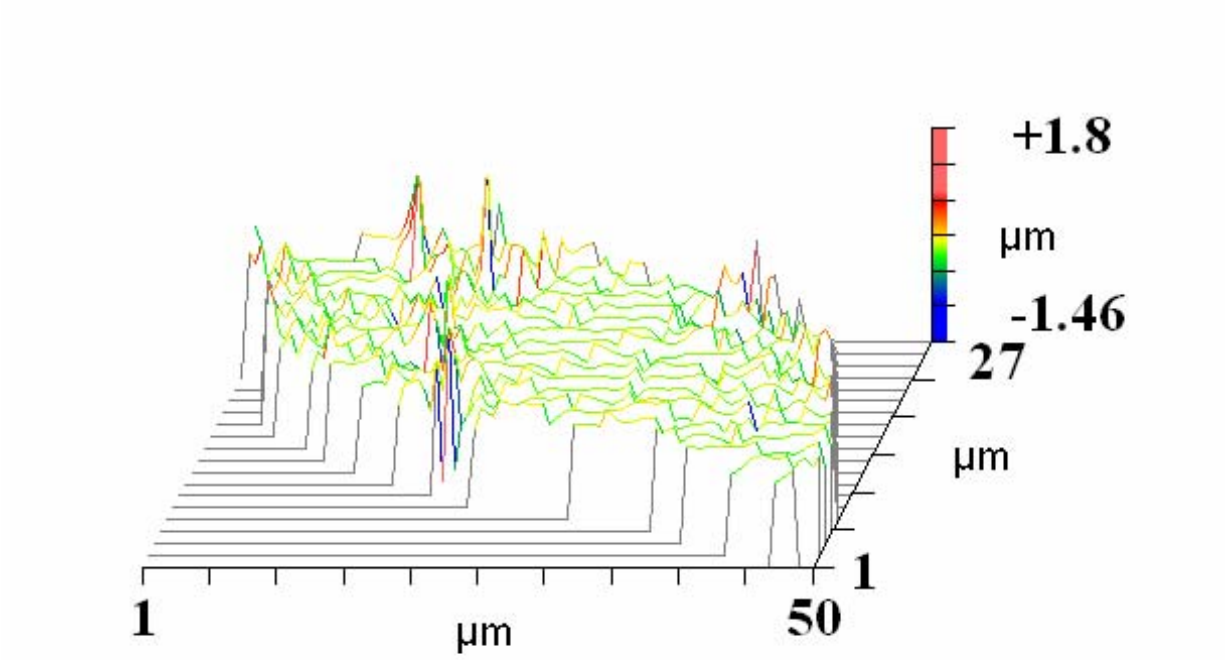

Figure 18. The figure shows an oblique plot representing a randomly chosen area on 1:1 PLGA-B-HA composite. The selected area is marked as shown by the arrow (Fig. 17). The thickness of the area varies from -1.46 to +1.8 µm. The negative sign indicates the valleys and the positive sign indicates the presence of peaks on the surface. The red lines indicate the presence of higher peak heights up to +1.8 µm and not too many peaks could be observed here. Majority of the peaks are approximately of height 1.6 µm are indicated by the green lines. The valleys correspond to the blue lines.

Fig. 19, Fig. 22 and Fig. 25 indicate the 2-d profiles of the selected areas corresponding to 1:1, 1:2 and 1:3 PLGA-B-HA composites. Fig. 19 shows the presence of narrower peaks.

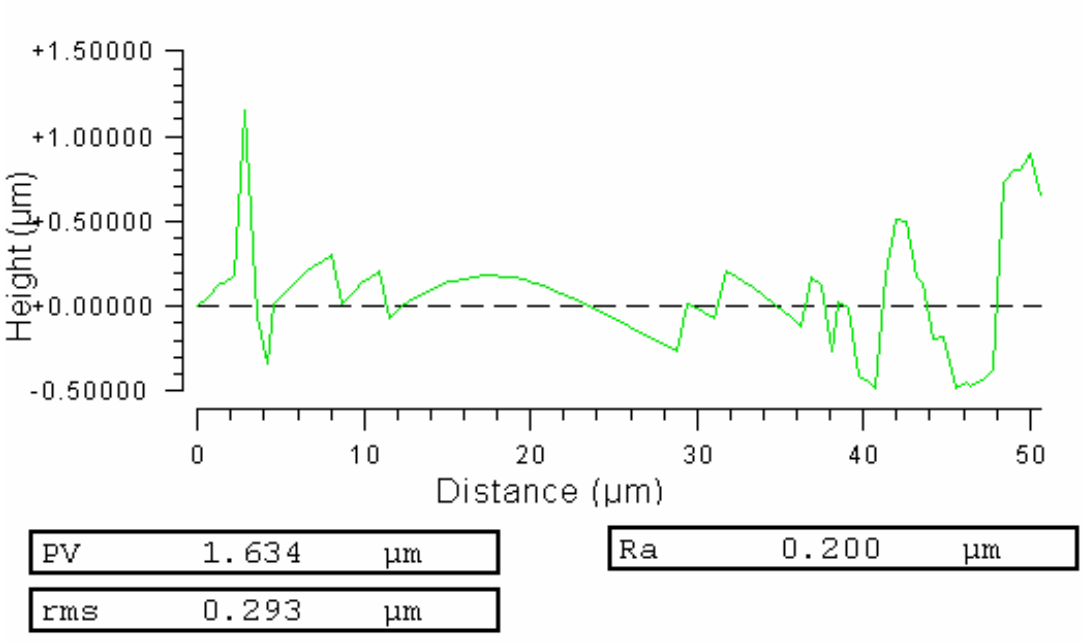

Figure 19. Figure indicates a 2-D profile of a randomly chosen area on 1:1 PLGA-B-HA composite as indicated by the arrow (Fig. 17). The figure indicates the presence of narrower peaks.

Figure 20. Represents the surface of 1:2 PLGA-B-HA composite. The arrow indicates the area to be scanned.

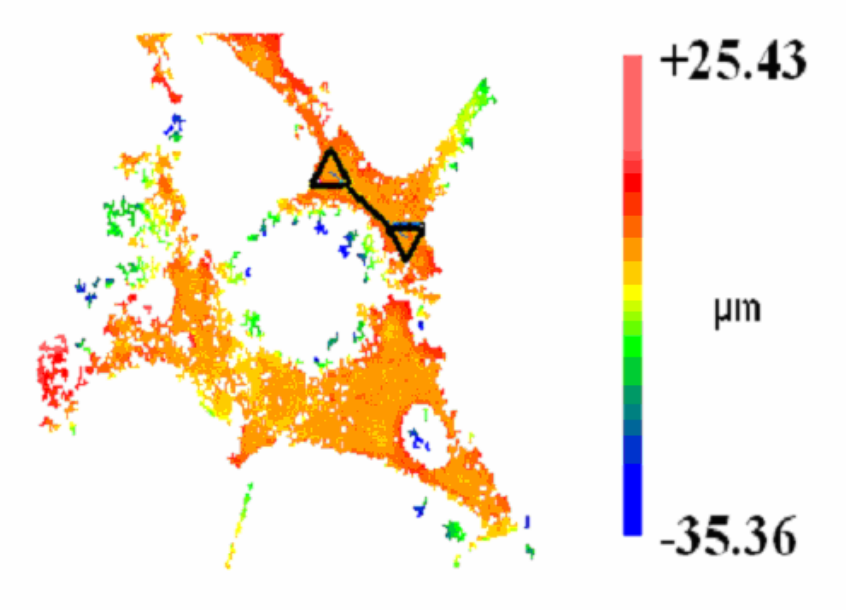

Figure 20. The color contour is represented by the micron scale and varies from -35.36 to + 25.43 µm. The positive value corresponds to the peaks whereas the negative value corresponds to the valleys. The peaks are indicated by the green, yellow and red areas. The valleys are indicated by the blue areas.

Fig.21 indicates the presence of larger number of peaks with a considerable increase in the peak heights ranging from -3.5 to +2.135 µ. Peaks are indicated by the green and red lines. The blue lines correspond to the valleys.

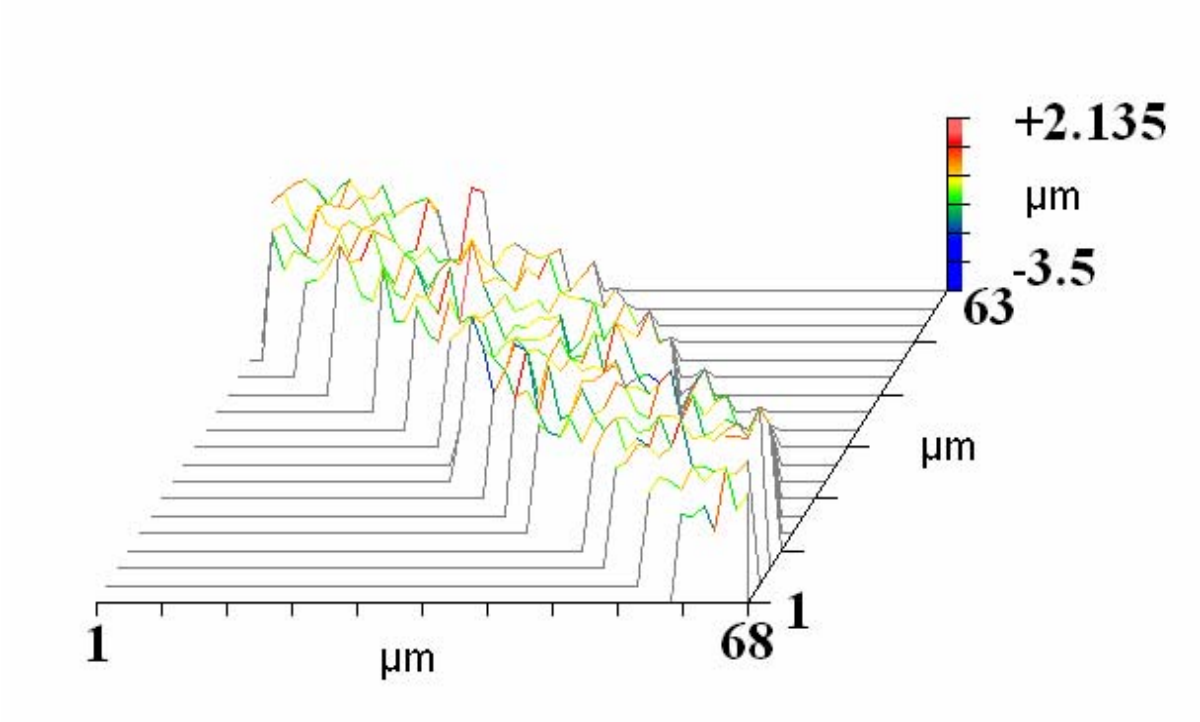

Figure 21. The figure shows an oblique plot of a randomly chosen area on 1:2 PLGA-B-HA composite. The selected area is marked as shown by the arrow (Fig.20). The thickness of the selected area varies from -3.5 to +2.135 µm. The negative sign indicates the valleys and the positive sign indicates the presence of peaks on the surface. Large number of peaks with increased peak heights up to 2.135 µm could be observed on 1:2 as compared to 1:1 PLGA-B-HA surface. The peaks are indicated by the red and green lines whereas the valleys correspond to the blue lines.

Fig. 22 showed an increase in the peak height and width as the ceramic concentration was increased as compared to 1:1 PLGA-B-HA composites.

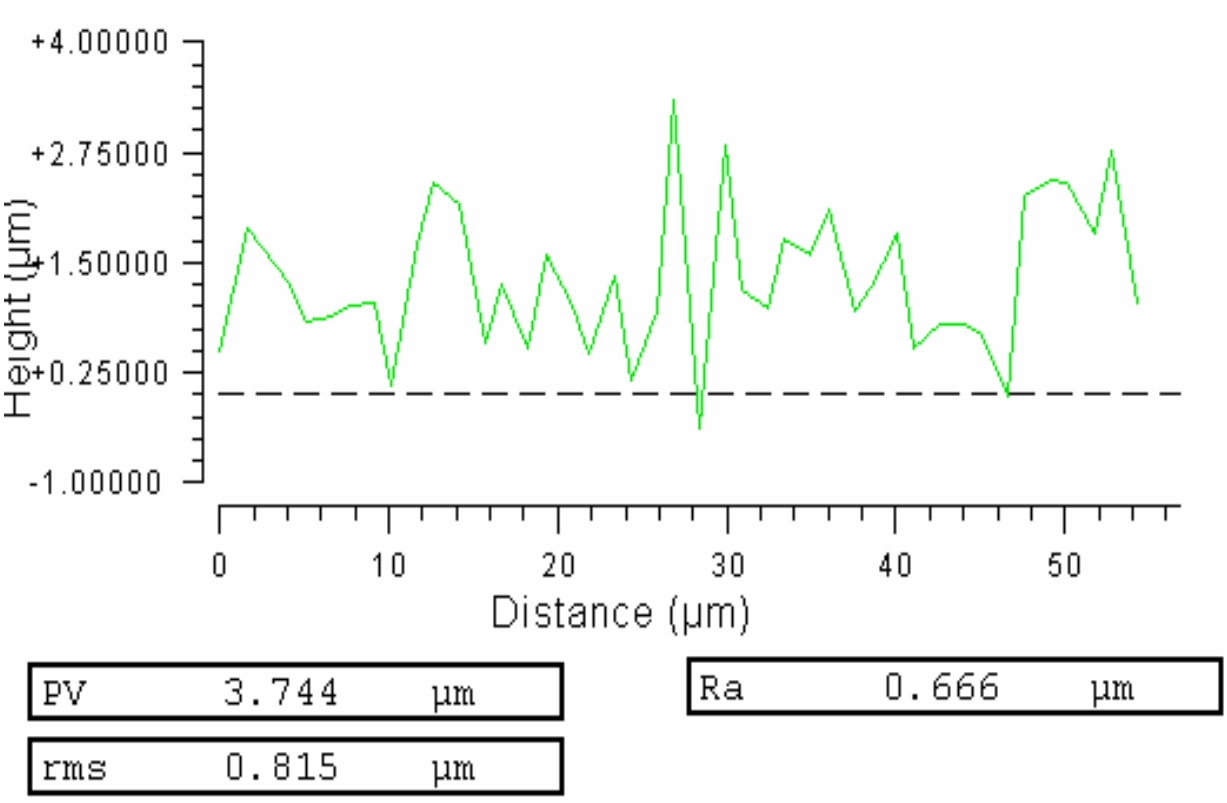

Figure 22. Figure indicates a 2-D profile of a randomly chosen area on 1:2 PLGA-B-HA composite as indicated by the arrow (Fig. 20). As the ceramic concentration was increased, an increase in the peak width and height up to 3.5 µm could be observed.

Fig.23. represents the surface of 1:3 PLGA-B-HA composite. The arrow indicates the area to be scanned.

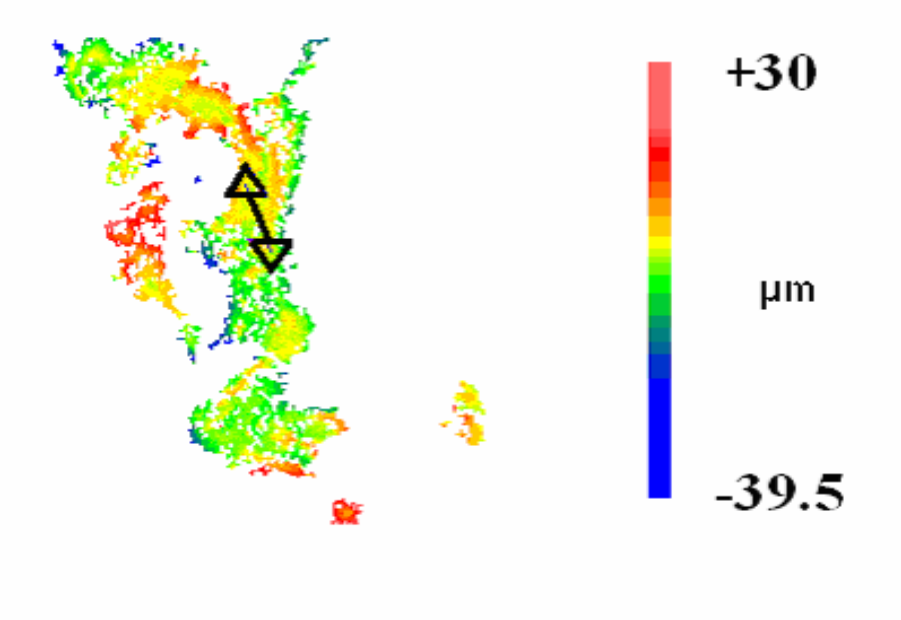

Figure 23. The color contour is represented by the micron scale and varies from -39.5 to +30 µm. The positive value corresponds to the peaks whereas the negative value corresponds to the valleys. The peaks are indicated by the green, yellow and red areas. The valleys are indicated by the blue areas.

Fig.24 indicates An increase in the number of peaks with heights varying from -2.8 to +2.065 µ and are indicated by the red, yellow and green lines on the 1:3 PLGA-B-HA surface. The valleys are indicated by the blue lines.

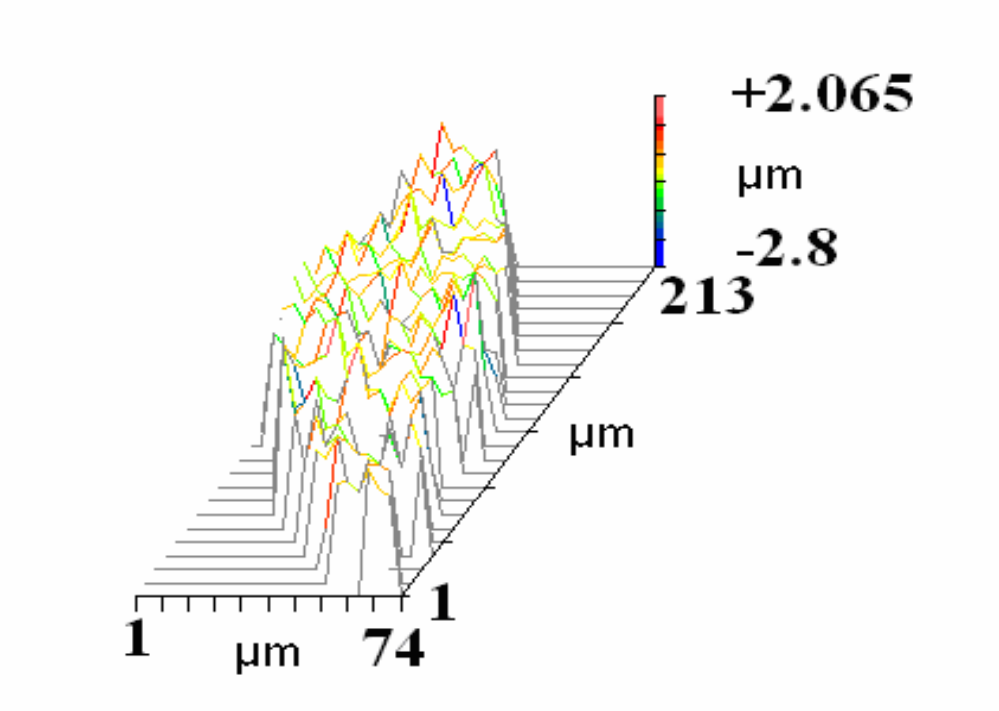

Figure 24. The figure shows an oblique plot of a randomly chosen area corresponding to 1:3 PLGA-B-HA composite. The selected area is marked as shown by the arrow (Fig. 23). The thickness of the selected area varies from -2.8 to +2.065 µm. The negative sign indicates the valleys and the positive sign indicates the presence of peaks on the surface. Here larger number of peaks with increased peak heights up to 2.065 µ could be observed. The surface appears to be rougher due to the increase in the number of peaks as compared to 1:1 and 1:2 PLGA-B-HA composites. The peaks are indicated by the red yellow and green lines. The valleys correspond to the blue lines.

Fig. 25 indicates a considerable increase in the peak heights and widths in case of 1:3 PLGA-B-HA composites.

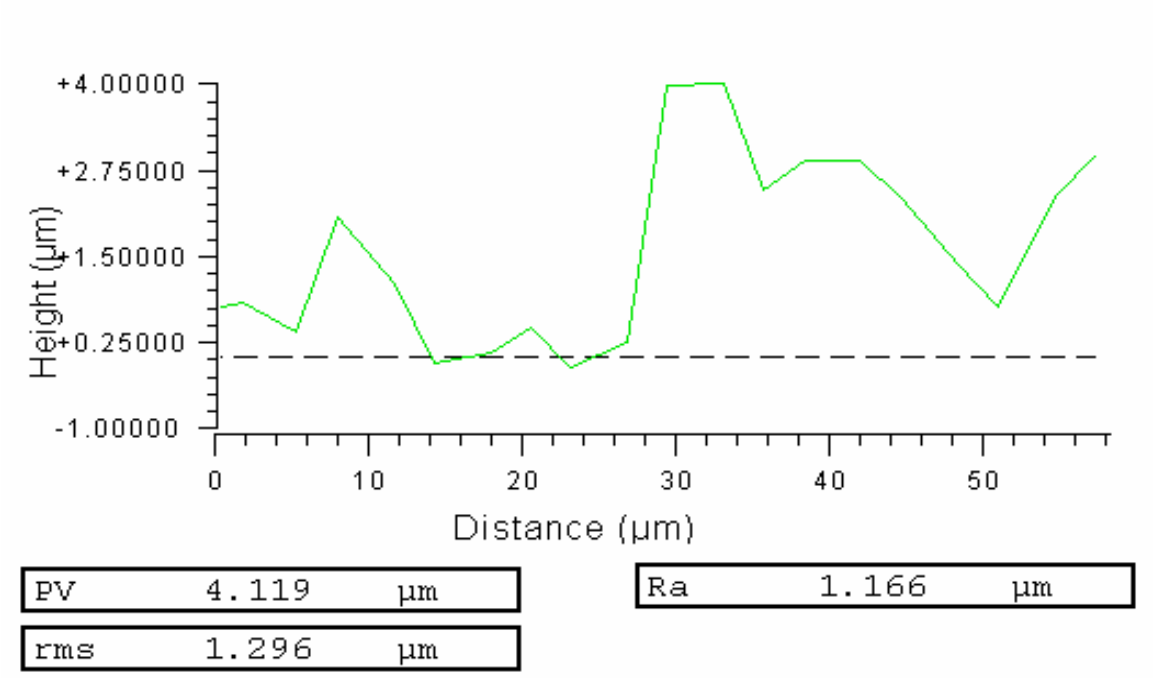

Figure 25. Figure indicates a 2-D profile of a randomly chosen area on 1:3 PLGA-B-HA composite as indicated by the arrow (Fig. 23). As the ceramic concentration is further increased a significant increase ($p < 0.05$) in the peak width and height up to 4 µm could be observed. After a certain scanning length i.e. between 30- 50 µ not many valleys could be observed.

The results indicate significantly higher ($p < 0.05$) average (Ra) values of roughness for 1:3 as compared to1:1 and 1:2 PLGA-B-HA composites (Table 2). The Ra values increased in the order 1:3 > 1:2 > 1:1.

SAMPLES	Ra (μM)	Rrms (μM)	SAMPLE COMPARISON	p-Ra	p-Rrms
1:1	5.022±3.364	6.77±4.406	1:1 &1:2	0.007	0.007
1:2	10.11±2.851	13.641±3.5	1:1&1:3	0.00024	0.00024
1:3	13.6±1.762	17.145±2.14	1:2 &1:3	0.0032	0.0032

Table 2. Indicates average roughness values of 1:1, 1:2 and 1:3 PLGA-B-HA composites respectively. The table also provides the statistical comparison of the average roughness values of 1:1, 1:2 and 1:3 PLGA-B-HA composites.

3.2.2 FTIR analysis

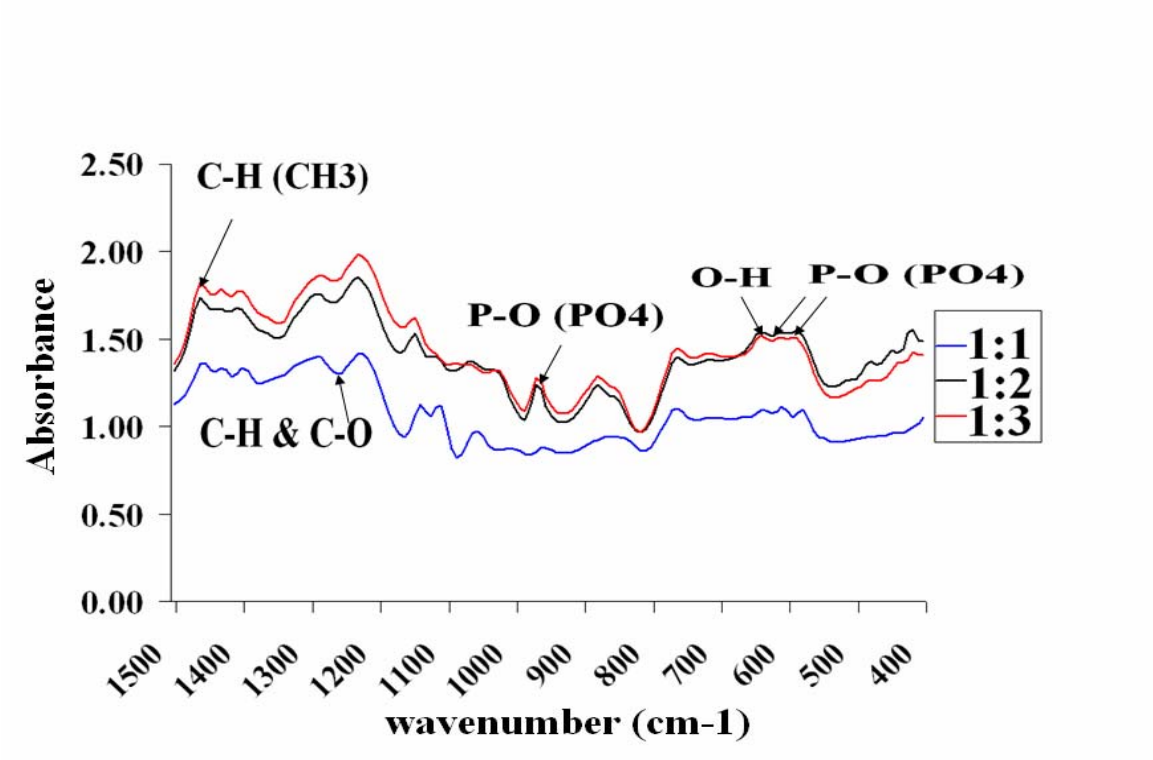

Figure 26. FTIR spectra of 1:1. 1:2 and 1:3 PLGA-B-HA composites. The functional groups corresponding to the polymer (PLGA) and ceramic (HA) are indicated in Table 3.

Table. 3 summarizes the IR bands corresponding to the polymer and the ceramic respectively. The areas under the ceramic and polymer peaks were analyzed and compared for 1:1, 1:2 and 1:3 PLGA-B-HA composites.

IR BANDS (cm^{-1}) (PLGA)	ASSIGNMENTS	IR BANDS (cm^{-1}) (HA)	ASSIGNMENTS
1453	C-H(CH_3) groups	1090,1042	P-O(PO_4) groups
1348,1388	C-H(CH_3) groups	962	P-O (PO_4) groups
1269	C-H and C-O	872	P-OH (HPO_4) groups
1189	C-O	627	O-H (OH) group
		602,567	P-O(PO4) groups
		471	P-O(PO4) groups

Table 3. Infrared vibrational frequencies of PLGA and HA in the 2000-1000 cm^{-1} and 2000-400 cm^{-1} region.

3.2.3 Mechanical testing

Table 4 summarizes the compressive modulus and failure strain of 1:1, 1:2 and 1:3 PLGA-B-HA composites respectively. The table also provides a comparison of compressive strengths and modulli of PLGA-PCL-HA, PLGA-HA and PLGA-PCL composites with trabecular bone. Both, the compressive modulus and compressive yield strength of 1:1 are significantly higher ($n = 3$, $p < 0.05$) than those of 1:2 and 1:3 PLGA-B-HA composites respectively. Compressive strength and compressive modulus of 1:2 are significantly higher ($p < 0.05$) than 1:3 PLGA-B-HA composites.

POLYMER-CERAMIC COMPOSITES	COMPRESSIVE STRENGTH	FAILURE STRAIN	COMPRESSIVE MODULUS
1:1	0.36±0.055	0.145±0.0035	2.5±0.32
1:2	0.07±0.026	0.16±0.007	0.42±0.15
1:3	0.045±0.02	0.15±0.013	0.3±0.12

Table 4. The compressive modulus and yield strength of 1:1, 1:2 and 1:3 PLGA-B-HA composites prepared from the freeze drying lyophillization technique.

3.2.4 Biochemical Assays

3.2.4.1 Total protein analysis

Minimal difference ($n = 4$, $p > 0.05$) in the protein concentration secreted by the bone marrow stem cells on to 1:1, 1:2 and 1:3 PLGA-B-HA composites could be observed at the end of 10 and 30 days (Fig. 27). At the end of 20 days cells attached to the surface of 1:2 and 1:3 PLGA-B-HA composites produced significantly ($p < 0.05$) higher protein concentration (µg/ml) as compared to 1:1 PLGA-B-HA composites. No significant difference ($p > 0.05$) in the protein concentration produced by the cells cultured on to 1:2 and 1:3 PLGA-B-HA composites at the end of 20 days could be observed.

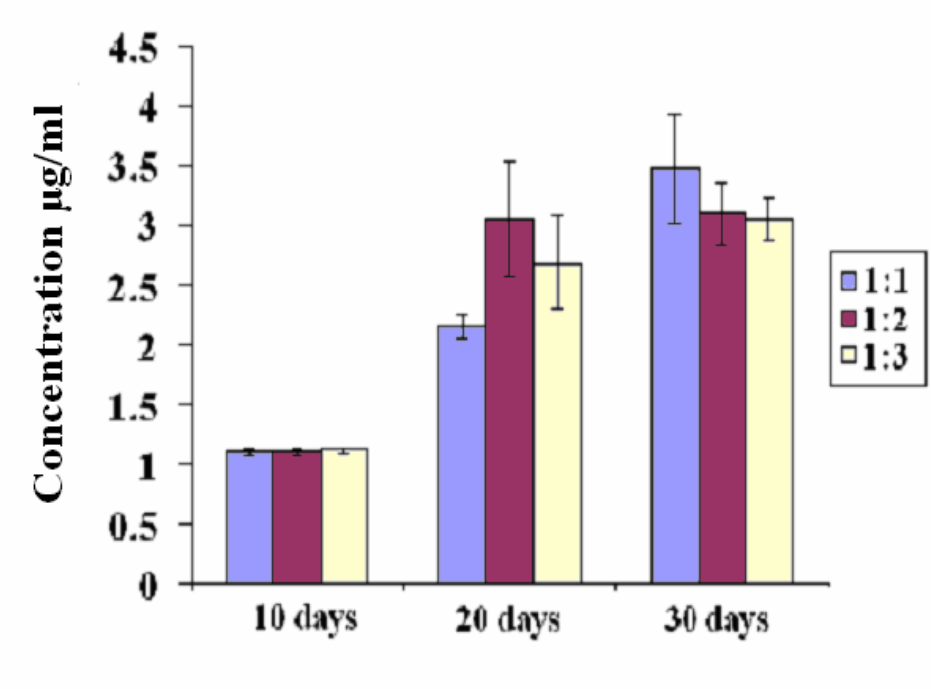

Figure 27. Indicates the concentration of the protein in µg/ml produced by the rat marrow cells cultured on to 1:1, 1:2 and 1:3 PLGA-B-HA composites at 10, 20 and 30 days respectively. The results show no significant difference in the protein concentration (µg/ml) produced by the cells cultured on to 1:1, 1:2 and 1:3 PLGA-B-HA composites at

the end of 10 days. At the end of 20 days, cells cultured on to 1:2 and 1:3 PLGA-B-HA surfaces produced significantly higher ($n = 4$, $p < 0.05$) protein as compared to 1:1 PLGA-B-HA surfaces. No significant difference ($p > 0.05$) in the protein concentration produced by the cells cultured on 1:2 and 1:3 PLGA-B-HA composites at the end of 20 days could be observed. At the end of 30 days no significant difference ($p > 0.05$) in the protein concentration produced by the cells cultured on 1:1, 1:2 and 1:3 PLGA-B-HA composites could be observed.

3.2.4.2 Alkaline phosphatase assay

Fig. 28 shows the AP activity in nmol of pNP/min/µg protein and protein concentrations produced by rat marrow cells cultured on to 1:1, 1:2 and 1:3 PLGA-B-HA composites for a period of 10, 20 and 30 days respectively. The results of the 10 and 20-day experiment indicated no significant difference ($n = 4$, $p > 0.05$) in the AP activities on 1:1, 1:2 and 1:3 PLGA-B-HA composites respectively. The results of the 30-day experiment indicated the bone marrow stem cells expressed significantly higher alkaline phosphatase ($n = 4$, $p < 0.05$) on 1:3 as compared to 1:1 and 1:2 PLGA-B-HA composites. No significant difference ($p > 0.05$) could be observed in the alkaline phosphatase activities of rat marrow stem cells on to 1:1 and 1:2 PLGA-B-HA composites at the end of 30 days respectively.

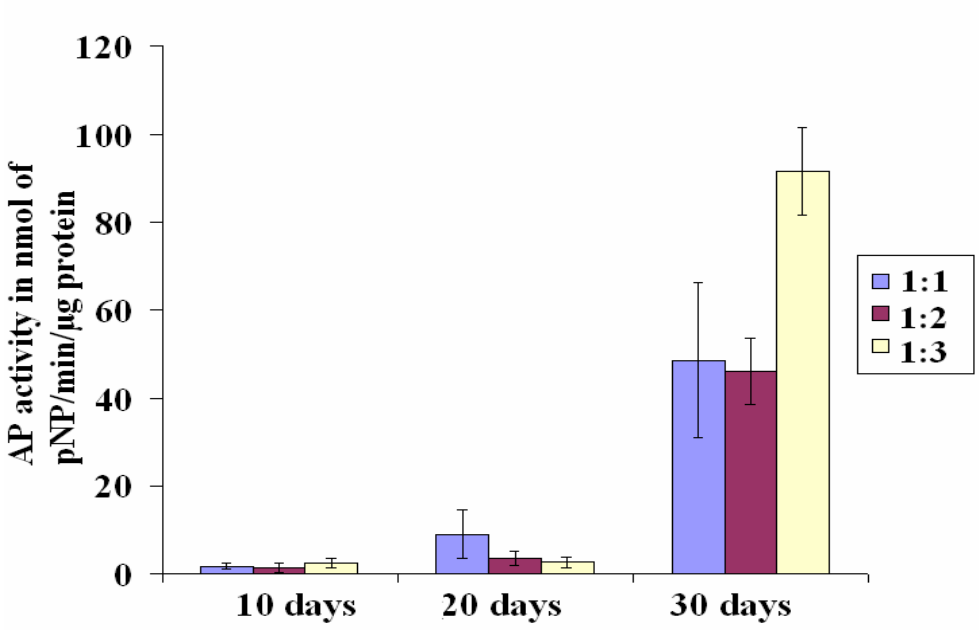

Figure 28. AP activity in nmol of pNP/min/µg protein produced by rat marrow stem cells on 1:1, 1:2 and 1:3 PLGA-B-HA composites at the end of 10, 20 and 30 days. The figure

represents the AP activity (nmol of pNP/min/µg protein) and protein concentrations (µg/ml) produced by rat marrow cells cultured on to 1:1, 1:2 and 1:3 PLGA-B-HA composites at the end of 10, 20 and 30 days respectively. At the end of 10 days, no significant difference ($n = 4$, $p > 0.05$) could be observed in the AP activity and protein concentrations on 1:1, 1:2 and 1:3 PLGA-B-HA composites. At the end of 20 days, no significant difference ($p > 0.05$) in AP activity produced by the cells on 1:1, 1:2 and 1:3 PLGA-B-HA composites could be observed. At the end of 30 days cells expressed significantly ($p < 0.05$) higher AP on 1:3 as compared to 1:1 and 1:2 PLGA-B-HA composites.

3.2.4.3Osteocalcin

Osteocalcin concentration in absorbance units of 1:1, 1:2 and 1:3 PLGA-B-HA composites and control samples were measured at the end of 14, 21 and 28 days respectively. The results indicated bone marrow stem cells seeded on to the 1:3 PLGA-B-HA composites expressed significantly higher (n =3, $p < 0.05$) osteocalcin at the end of 14 and 21 days respectively. 1:2 expressed significantly higher ($p < 0.05$) osteocalcin secretion by osteoblasts at the end of 28 days as compared to 1:1 PLGA-B-HA composites and 1:3 PLGA-B-HA composites. Cells seeded on to the 1:1 PLGA-B-HA composites produced significantly lower ($p < 0.05$) osteocalcin as compared to 1:2 and 1:3 PLGA-B-HA composites at the end of 28 days respectively (Fig. 29).

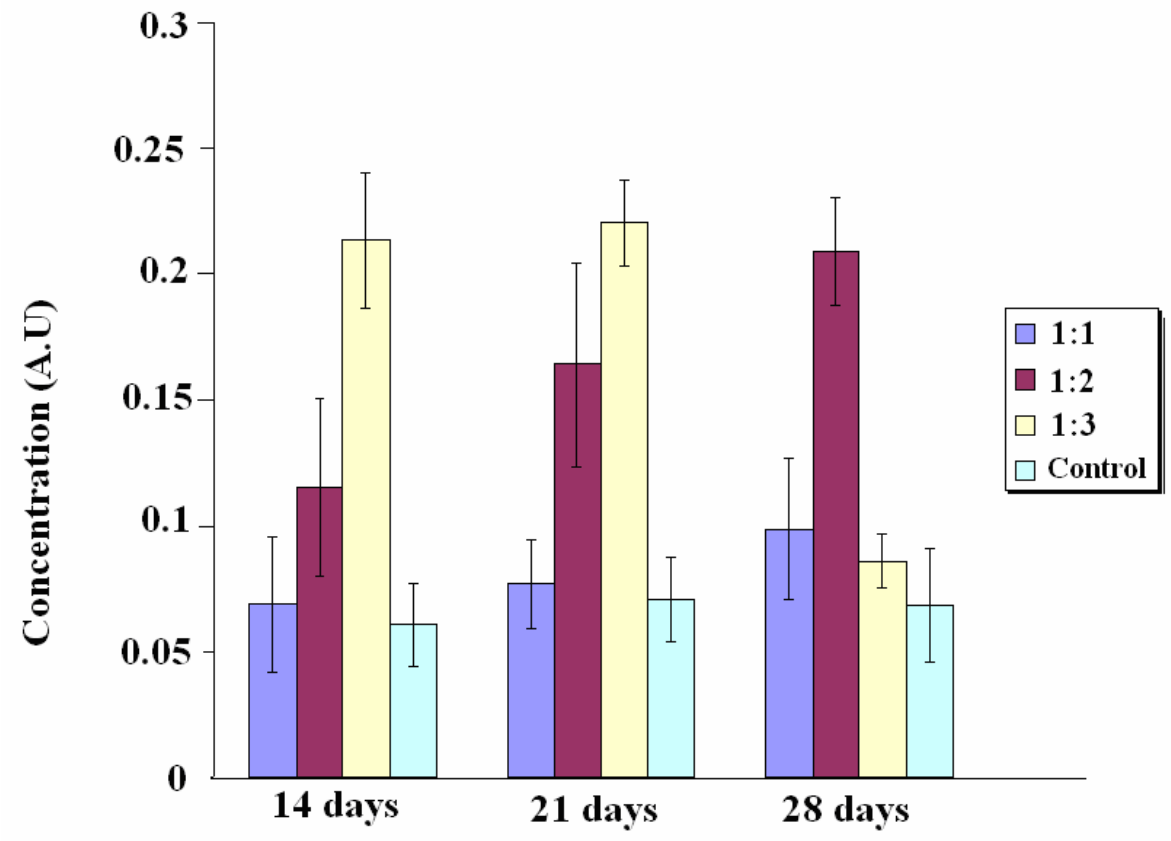

Figure 29. Osteocalcin concentration in absorbance units of 1:1, 1:2, 1:3 PLGA-B-HA composites and control samples at the end of 14, 21 and 28 days respectively.

3.2.5 Corrosion studies in tissue culture medium

3.2.5.1 Ca concentration at the end of 28 days

ICP analysis showed minimal difference (n = 4, $p > 0.05$) in the Ca concentrations of the tissue culture media incubated with or without various PLGA-B-HA samples at the end 7, 14, 21 and 28 days (Fig. 30).

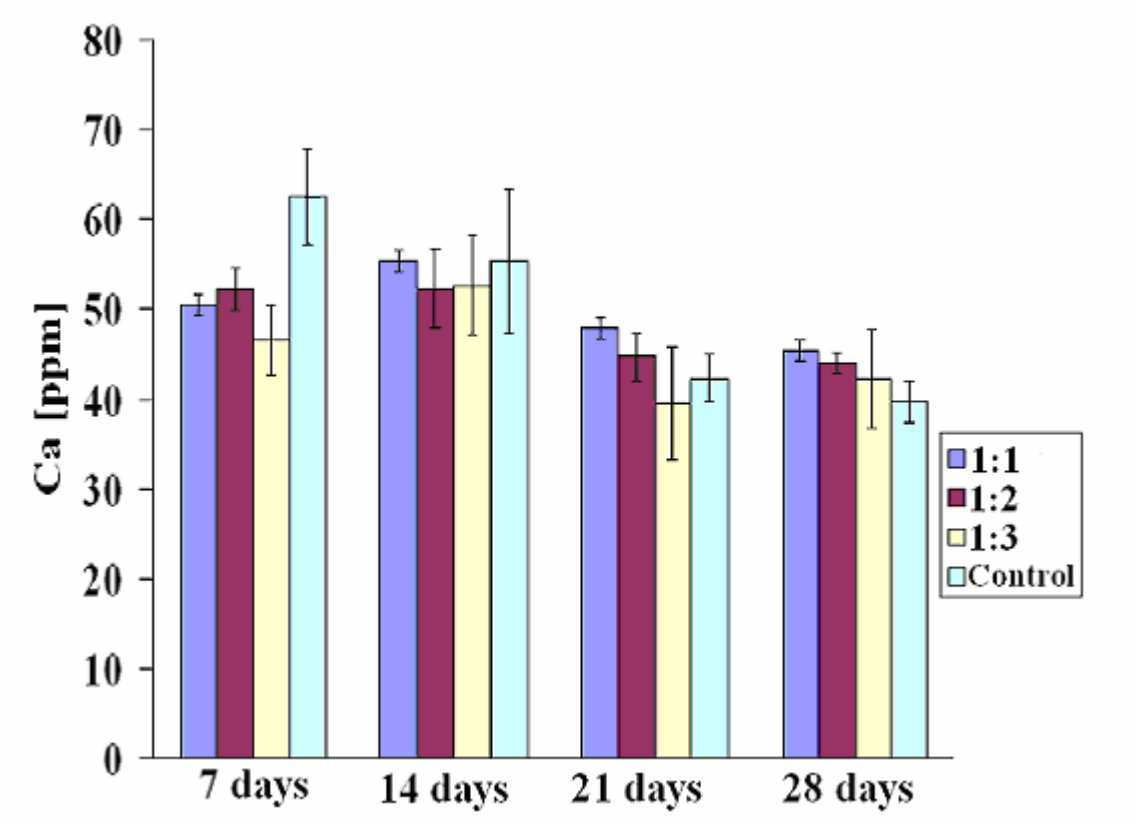

Figure 30. ICP measurements of Ca concentrations in the media incubated with PLGA-B-HA composites (1:1, 1:2, 1:3) and control samples incubated in polystyrene culture dishes for 7, 14, 21 and 28 days respectively in the presence of bone marrow stem cells.

3.2.5.2 P concentration at the end of 28 days

ICP analysis showed minimal difference (n = 4, p > 0.05) in the P concentrations between the PLGA-B-HA composites and cells incubated in polystyrene dishes at the end 7, 14, 21 and 28 days respectively (Fig.31)

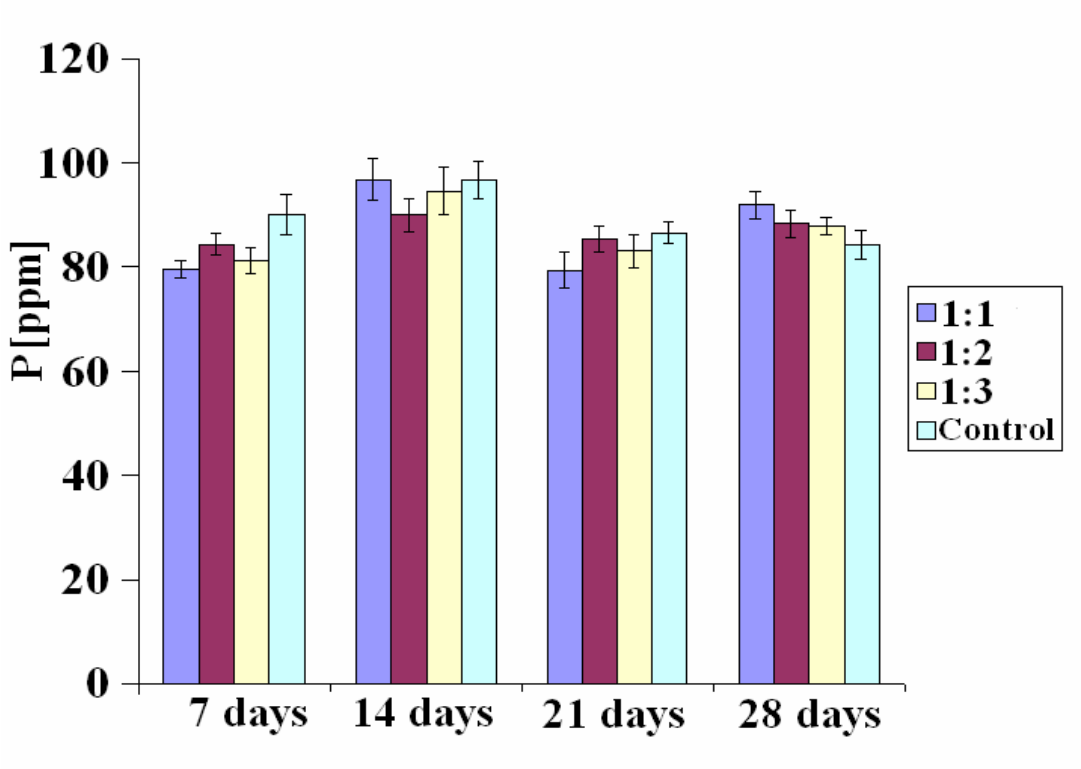

Figure 31. ICP measurements of p concentrations in the media incubated with PLGA-B-HA composites (1:1, 1:2, 1:3) and control samples incubated in polystyrene culture dishes for 7, 14, 21 and 28 days respectively in the presence of bone marrow stem cells.

3.2.6 pH measurements at the end of 28 days

pH values of 1:1, 1:2, 1:3 PLGA-B-HA composites and control samples incubated in polystyrene dishes in the presence of bone marrow stem cells at the end of 7, 14, 21 and 28 days respectively were measured. Results indicate a minimal difference ($p > 0.05$) in the pH values of the composites and cells incubated in polystyrene dishes in tissue culture medium at the end of 28 days (Table 5).

COMPOSITIONS 21^{ST} DAY	MEAN ± STDV. 21^{ST} DAY	COMPOSITIONS 28^{TH} DAY	MEAN ± STDV. 28^{TH} DAY
1:1	7.67 ± 0.06	1:1	7.5 ± 0.051
1:2	7.7 ± 0.042	1:2	7.54 ± 0.042
1:3	7.6 ± 0.1	1:3	7.62 ± 0.07
CONTROL	7.7 ± 0.14	CONTROL	7.33 ± 0.053

Table 5. pH values of the tissue culture media containing 1:1, 1:2, 1:3 PLGA-B-HA composites and control samples incubated in polystyrene dishes at the end of 21 and 28 days respectively**.**

CHAPTER FOUR

DISCUSSION

4.1 Pilot study

4.1.1 Significance of Bovine bone hydroxyapatite

To engineer an ideal scaffold has prompted us to synthesize a macroporous polymer-ceramic composite with an appropriate ratio of the bioresorbable polymer to the bioactive ceramic that could enhance osteoblast function. In our study we have employed porous bovine hydroxyapatite to synthesize the polymer-ceramic composite.

4.1.2 Significance of the copolymer ratio

The polymer used in the study was PLGA 50:50; Mw = 72000Da. The polymer was chosen due to controlled degradation and good mechanical properties. Degradation rate of the polymer can be controlled by altering the copolymer ratio and the molecular weights. Below a molecular weight of 10,000, PLGA foams had very little mechanical strength [57].

4.1.3 Significance of Freeze-drying technique

The PLGA-BHA composite synthesized using the Freeze-drying lyophilization technique [43-46, 57-60] allowed for highly porous structure with a pore size varying from 40-1000 μm as indicated by the arrows in (Fig. 1). In this procedure, two phases- a polymer-rich phase and a polymer-lean phase are formed by cooling down the polymer solution thereby inducing a liquid-liquid phase separation. The solvent is then extracted by placing it in a vacuum chamber and the solvent removal leads to the formation of the

macropores. Chloroform was preferred instead of dioxane due to its lower freezing temperature. As the ceramic concentration was increased, foams synthesized using dioxane as a solvent were rigid and microporous. The optimal pore size for bone grafting is in the range of 100-350 μm [43]. The PLGA-BHA material prepared in the present study satisfies most the requirement of the ideal pore size for osteoblasts infiltration, viability and function. SEM analyses indicated that PLGA-composite is marcoporous and had interconnected open pore morphology. SEM (Fig 7.) analysis indicated that neonatal rat calvaria osteoblasts attached to the surface of PLGA-B-HA. Also the composite is highly porous with the porosity varying from 30-1000 μ. This matches the requirement of the ideal pore size required for the promoting osteoblast viability and function.

4.1.4 Significance of cell-material interactions

Cell adhesion is an important aspect of cell interaction with a biomaterial since it is required for cell proliferation, differentiation and cell spreading on to the material surface. Cell adhesion and spreading are two distinct phenomenon's because it has been shown that the substrates that allow cell adhesion do not necessarily promote cell spreading. The initial osteoblast/material interactions are characterized by four stages: (1) protein adsorption to the surface, (2) contact of cells with the surface, (3) cell attachment and (4) cell spreading. The 90-min time would reflect the interactions involving the first contact of the cell with the substrate followed by the attachment on the substrate. Initial spreading occurs at the end of 4h which is characterized by reorganization of the cytoskeletal matrix and flattening of the cell. At the end of 24 hours the cells are expected to be flat and spread and to have started proliferating. There are no fixed time periods that

characterize the cell morphology as the cell morphology changes with the type of the substrate and also the type of the cell used [61].

After attachment to the PLGA-BHA the cells produced extensive mineralized ECM at the end of 2 weeks. The EDX ratio (Fig. 8, Fig. 10 and Fig. 12) indicates the presence of biological HA with the Ca/P ratio equal to 1.66. On the other hand (Fig. 5) indicated the cells on HA discs produced collagenous matrix. Also in some areas we could observe the collagen fibers merging to form a continuous sheet of ECM (Fig. 6). However, no inorganic matrix was produced by the cells attached to HA which could be seen by the absence of calcified nodules. While the HA discs stimulated the formation of un mineralized organic matrix, the PLGA-B-HA composites stimulated both the formation of organic as well as the inorganic matrix. This could be seen by the presence of calcified nodules (Fig. 7 and Fig. 9). Cells appear to be somewhat flat when cultured on to the surface of PLGA/PCL/HA composites at the end of 2 weeks [62].

However in our study we observed comparatively extensive mineral secretion by neonatal rat calvarial osteoblasts cultured on to PLGA-B-HA composites at the end of 2 weeks. The results of the pilot study indicated higher cellular activity on PLGA-B-HA composites as compared to pure HA discs. Higher osteoconductivity of B-HA is due to the similar mineral content or inorganic portion of the ceramic as that of the bone. Even though the inorganic component of Interpore 200 is similar to that of the inorganic portion of natural bone, the porosity when compared to B-HA is different. We have evaporated the organic component from the bovine bone thereby leading to the formation

of a porous structure. The porosity of the ceramic (B-HA) provides larger surface area thereby increasing cell attachment, facilitating cell infiltration and extracellular formation as observed from the SEM (Fig. 8 and Fig. 10). .

Hence the results of the pilot study have prompted us to further expand and evaluate the effect of varying the ceramic concentration on the stimulation of osteoblastic activity.

4.2 Main study

4.2.1 Significance of surface topography

Surface modification of biomaterials has been one of the major factors in the development of tissue engineering. As a scaffold, the significance of biomaterials is that they can not only interact with the cells but also with the host environment, through the interface. Immobilization of bioactive molecules on the surface of the substrate would mediate cell behavior. Such differences in topographies contribute to the changes in hydrophobicity/hydrophilicity balance. On the other hand, such differences also led to the differences in deposition of serum proteins. It is generally known that the hydrophobicity/hydrophilicity of a film surface can affect the degree of cell adhesion and proliferation. Hydrophilicity is a factor affecting surface energy, which might influence serum proteins that adhered to these materials and in turn influence cell proliferation and differentiation [61]. It has been observed that the topography of a porous surface enhances migration by physically directing tissue movement [62].

Lactic acid is more hydrophobic than glycolic acid, and increase in its concentrations increases hydrophobicity. An increase in hydrophobicity corresponds to the decrease in degradability. PLGA is amorphous in nature and hence the copolymer matrices degrade at a relatively high rate. An increase in PLA or PGA content in PLGA will increase the crystallinity of the polymer and hence the degradation time [64]. Migration of the cells on to the porous surface was dependent on the surface chemistry. It has also been reported that hydrophilic surfaces exhibit greater cellular adhesion over hydrophobic surfaces [64-66]. Sato et al. showed exposure of HA and/or TiO_2 particles in PLGA+TiO_2 precursor+HA coatings after decomposition of PLGA due to hydrolysis increased coating hydrophilicity [67]. Also it has been reported that surface roughness leads to an increase in adhesion of bone forming cells, indicating the remodeling activity [67-72]. Schwartz et al. studied that the microrough topography of titanium implants exhibited increased pull out strength *in vivo* suggesting increased implant-tissue adhesion. *In vitro* studies further revealed that as the surface microroughness is increased, osteoblast proliferation is decreased whereas differentiation is increased [72]. Anselme et al. qualitatively evaluated the adhesion of human osteoblasts on orthopedic metallic substrates with various surface roughnesses and its correlation with qualitative changes in the expression of adhesive proteins and with parameters describing the surface topographies [73]. It was shown that the cell layer organization was modified by the roughness of the material surfaces thereby initiating cell differentiation [73-75].

4.2.2 Effect of the chemical composition on the morphology of 1:1, 1:2 and 1:3 PLGA-B-HA composites

4.2.2.1 Surface roughness characterization

4.2.2.1.1 Qualitative analysis of surface roughness

Fabrication parameters such as ceramic to polymer concentration and water to solvent ratio were varied to arrive at reproducible targeted macroporous structures. From the SEM we can clearly observe a difference in the pore wall thickness and porosity in case of 1:1, 1:2 and 1:3 PLGA-B-HA composites (Fig. 13, Fig. 14 and Fig. 15). A significant increase ($p < 0.05$) in the pore wall thickness in the order of 1:3 > 1:2 > 1:1 could be observed (Table 1). The thicker pore walls of 1:3 PLGA-B-HA may be due to the higher concentration of the ceramic. There might be due to the ceramic particles that are loosely adhered on to the pore walls of the composite. We could observe an increase in ceramic concentration decreases the porosity as observed in case of 1:3 PLGA-B-HA composites. This is due to the decrease in the volume of the solvent due to the increase in ceramic concentration.

4.2.2.1.2 Quantitative analysis of surface roughness

Characterization of the changes in surface topography was done using the "New View 5000" scanning white light interference microscope. For analyzing the changes in surface topography the sample surface has to be extremely reflective. Specific regions within a reflective surface are selected and are converted to corresponding data points thereby creating an image which is eventually displayed on a computer screen. Certain areas were selected on the surface of 1:1, 1:2 and 1:3 polymer-ceramic composites respectively (Fig.

16, Fig. 19 and Fig. 22) and by a command called 'MASK' we highlighted the specific areas and captured the 2-D and 3-D profiles respectively. We have analyzed 10 different areas on the pore walls of different compositions (1:1, 1:2 and 1:3 respectively) and computed the average, rms and peak roughness values. The average, peak and the rms values varies position by position on the sample surface indicating a change in the topography.

The results indicate that the average roughness values (μm) in the order of 1:3 > 1:2 > 1:1. Table 1. indicates a significant increase ($n = 3$, $p < 0.05$) in the pore wall thickness in the order of 1:3 > 1:2 > 1:2 PLGA-B-HA composites. Fig. 17, Fig. 20 and Fig. 23 indicate an oblique plot of a specific area (Fig. 16, Fig. 19 and Fig. 22) on 1:1, 1:2 and 1:3 PLGA-B-HA composites respectively. The peaks are indicated by the red and the green lines whereas the valleys are indicated by the blue lines. As the concentration of the ceramic is increased an increase in the area under the peak is observed. The scanning depth on the surface was 50 μm. The maximum peak height from the line profile for 1:1 was 1 μm, whereas for 1:2 and 1:3 it was 3.4 and 4 μm respectively. As the concentration of the ceramic is increased due to deposition of ceramic on to the surface, the height of the peak is increased as seen by the 2-D profile with an increase in the width (Fig. 18, Fig. 21, and Fig. 24). The increased width represents the increased ceramic concentration thereby covering some valleys.

Pore wall roughness indicates a variation in surface topography. Higher variation in topography gives a higher peak to valley value. Also higher Ra value indicates higher

roughness. 2-D profiles quantify the roughness and compare the changes in topography on different areas within the same sample as well within different samples. 1:1 represents a comparatively smoother surface indicating lesser magnitude of the peak to valley distance. 1:2 indicates a significantly higher peak to valley distance indicating a bumpier surface as compared to 1:1. When analysis was done on 1:3 PLGA-B-HA composite it showed significantly higher ($p < 0.05$) roughness as compared to 1:2 and 1:1 PLGA-B-HA composites respectively. The surface roughness was increased due to the ceramic concentration. Ceramic (B-HA) is rough in nature and an increase in ceramic concentration led an increase in surface roughness. Niederauer et al. showed that surface roughness, for osteoceramic materials, improved surface wetting properties [76]. This can further promote cell adhesion on to the biomaterial via formation of focal contacts or indirectly through selective adsorption of osteoinductive proteins favoring cell adhesion. The surface energy of hydroxyapatite significantly influences cell adhesion and spreading of human osteoblastic cells at the surface [77]. Hence an increase in hydroxyapatite concentration is indicated by the increase in the surface roughness. An increase in surface roughness contributes to the increase in the surface area thereby favoring cellular attachment.

4.2.3 FTIR analysis

Table 3 indicates the characteristic peaks in the region 1500-1000cm^{-1} and 1000-400 cm^{-1} for the polymer and hydroxyapatite respectively [78]. FTIR analysis indicated the presence of the ceramic phase as observed by the characteristic bands of PLGA and HA (Fig. 25). An increase in the area under the ceramic phase could be observed in case of 1:3 as compared to 1:1 and 1:2 PLGA-B-HA composites.

The results indicate an increase in the ceramic concentration, increases the area under the ceramic peak thereby increasing the ratio of the area measured under the ceramic to polymer (Fig. 25). The IR bands corresponding to the ceramic peaks are located at 567, 602 cm^{-1} and 962 cm^{-1}, representing the P-O (PO_4) groups and 627 cm^{-1} representing the O-H groups respectively. The IR bands corresponding to the polymer peaks are located at 1453 cm^{-1} representing C-H (CH_3), C-H and at 1269 cm^{-1} corresponding to C-O groups respectively. In the above study we have incorporated PLGA in to B-HA to modify the degradation as well as to improve the mechanical properties of the composite

4.2.4 Mechanical testing

For mechanical testing 3 samples were tested for each composition. The samples were tested under compression. It was observed that the compressive strength and modulus of 1:1 were significantly higher than those of 1:2 and 1:3 PLGA-B-HA composites. The polymer-ceramic composite is synthesized using the freeze drying/lyophilization technique. The polymer in this case forms a supporting matrix to which the ceramic particles adhere. An increase in the ceramic concentration or a decrease in the polymer

concentration gives rise to loosely attached ceramic particles. The particles are loosely bounded and have a tendency to shed off from the surface of the composite. For 1:2 and 1:3 PLGA-B-HA composites significant leaching of the ceramic particles could be observed. Hence this lowers the ceramic concentration and as the polymer concentration is less as compared to 1:1 PLGA-B-HA composites, we could observe a significant decrease in the compressive strengths and modulli of 1:2 and 1:3 PLGA-B-HA composites. The results indicate that the optimal ratio between the polymer and the ceramic is important in improving the mechanical properties, particularly the mechanical strengths. The composite will allow us to modify the mechanical properties by optimizing the molecular weights and the ratio of the polymer to the ceramic incorporated during the fabrication process.

4.2.5 Bioactivity evaluation

4.2.5.1 Alkaline phosphatase assay

Alkaline phosphatase activity is a characteristic marker of early osteoblastic differentiation. We have analyzed the alkaline phosphatase activity of bone marrow stem cells cultured on to 1:1, 1:2, 1:3 PLGA-B-HA composites and control samples incubated in polystyrene dishes immersed in tissue culture media over a period of 10, 20 and 30 days. A significant difference ($n = 4$, $p < 0.05$) in the AP activity of 1:3 over 1:1 and 1:2 PLGA-B-HA composites at the end of the 30-day period whereas no significant difference ($p > 0.05$) were observed at the end of 10 and 20 days (Fig. 28). Protein concentration (μg/ml) indicates no significant difference ($p > 0.05$) secreted by the rat

marrow stem cells on 1:1, 1:2 and 1:3 PLGA-B-HA composites at the end of 30 days (Fig. 27).

Tiffitt et al. showed the alkaline phosphatase staining demonstrated stimulation of this marker of the osteogenic phenotype in the cultures grown with the cements compared with human bone marrow stem cells cultured on plastic alone [79]. The results indicated that alkaline phosphatase produced by cells increased significantly when grown in the presence of calcium phosphate cements. Enzyme expression was increased in cells in contact with the surface of the carbonated apatite and 90% hydroxyapatite cements as compared to cells grown on plastic alone.

4.2.5.2 Osteocalcin

Osteocalcin or BGP (bone gla protein) is exclusively found in bone tissue. It accounts for 10-20% of the non-collagenous protein in bone. While the *in vivo* function of osteocalcin is unknown, its affinity for bone mineral constituents implies a role in bone formation [80]. It is a characteristic marker of bone forming cells i.e. osteoblasts. Cells attached on to the surface of 1:3 PLGA-B-HA composites produced significantly higher osteocalcin as compared to 1:1 and 1:2 composites (Fig. 32). Also, here we could observe the cells produced osteocalcin at a relatively shorter period i.e. 14 days of time on the 1:3 as compared to 1:2 and 1:1 PLGA-B-HA composites respectively (Fig. 30). Cells produced higher osteocalcin on 1:2 PLGA-B-HA composites at the end of 28 days. At the end of 28 days we could observe a significant decrease ($p < 0.05$) in the osteocalcin concentration in 1:3 PLGA-B-HA composites. No significant difference ($p < 0.05$) in the

osteocalcin concentrations could be observed on 1:1 PLGA-B-HA composites and cells incubated in polystyrene dishes at the end of 28 days respectively.

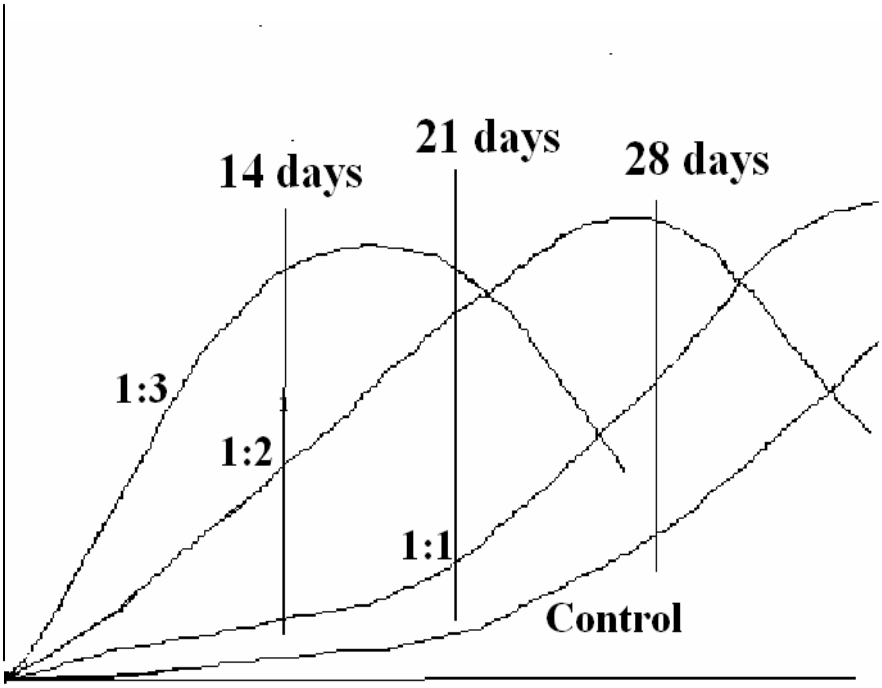

Figure 32. Indicates the osteocalcin concentration on 1:3 PLGA-B-HA composites at a relatively short period of time as compared to 1:1, 1:2 PLGA-B-HA composites and control samples at the end of 14, 21 and 28 days respectively**.**

Osteocalcin concentration produced by the cells on to 1:3 is significantly higher at the end of 14 days as compared to 1:2 and 1:1 PLGA-B-HA composites. Cells seeded on to 1:3 PLGA-B-HA composites secreted higher osteocalcin and at a shorter period of time as compared to 1:2 and 1:1 PLGA-B-HA composites (Fig.32). Also cells seeded on to 1:2 PLGA-B-HA composites secreted higher osteocalcin at the end of 21 days whereas no increase in osteocalcin could be observed for the cells seeded on to 1:1 and cells cultured

in polystyrene dishes at the end of 30 days respectively. Hence it could be inferred that a higher ceramic (B-HA) concentration stimulates osteoblastic differentiation. Ma et al. studied the synthesis of highly porous biodegradable polymer-hydroxyapatite scaffolds. The results indicated that HA is osteoconductive and porous PLLA/HA scaffolds are superior to pure PLLA scaffolds for bone tissue engineering [43]. Cellular activity was determined using osteocalcin and bone sialoprotein measurements in tissue culture medium followed by DNA assay analysis. The osteocalcin concentration produced by the cells was high on to PLLA/HA scaffolds as compared to the PLLA scaffolds at the end of 6 weeks. In our study the results indicated, higher ceramic concentration as in the case of 1:3 PLGA-B-HA composite stimulated osteocalcin secretion at the end of 14 days. This indicates stimulation of osteoblast function at an earlier time period which is due to the increase in bovine hydroxyapatite concentration in the composite material.

4.2.6 Corrosion studies in tissue culture medium

ICP analyses indicate a minimal difference in Ca and P concentrations from 1:1, 1:2, 1:3 PLGA-B-HA composites and control samples incubated in polystyrene dishes ($p > 0.05$) at the end of 7, 14, 21 and 28 days respectively (Fig. 30 and Fig. 31). From this we can infer that there was a minimal difference in the dissolution/precipitation of Ca and P from the degradation of PLGA-B-HA composites and that secreted from the osteoblasts. This also indicates that the concentration of Ca and P due to the degradation of PLGA-B-HA composite was similar to the Ca and P concentration produced by the activity of the bone marrow stem cells. Hence the presence of the PLGA-B-HA composite did not affect the ionic concentration of Ca and P.

The corrosion products of the material can deteriorate the cell activity due its toxicity effect or the adverse effect on pH. An increase or decrease in the environmental pH could be unfavorable to the cells and could hinder cell attachment and hence bone formation. The ideal pH value for tissue culture medium at 37^0C is 7.4. The pH values were measured at 25.2^0C. No significant difference in pH was observed at the end of and 28 days for PLGA-B-HA composites and control samples respectively (Table 5). Most importantly no significant difference ($p > 0.05$) could be observed in pH values for 1:1, 1:2, 1:3 PLGA-B-HA composites and control samples incubated in polystyrene culture dishes at the end of 28 days were observed. Hence the presence of the composite did not affect the pH of the surrounding environment.

CHAPTER FIVE

CONCLUSIONS

1. We have engineered a novel porous B-HA-polymer ceramic composite and correlated the effect of an increase in ceramic concentration on to stimulation of mesenchymal stem cells to restrict to osteoblastic phenotypes.
2. PLGA-B-HA composites were highly porous with an interconnected porous network which enhanced cell colonization.
3. Composites with high ceramic concentration induced osteoblast differentiation as indicated by high AP activity, high osteocalcin concentration, and mineralized extracellular matrix formation.
4. Increased surface roughness enhances cellular activity as indicated by 1:3 PLGA-B-HA composites**.**
5. The presence of the PLGA-B-HA composite did not affect the ionic concentration of Ca and P and the surrounding pH.
6. A variation in the chemical composition affected the cellular activity of osteoblasts.
7. An increase in ceramic concentration stimulated osteoblast function.
8. PLGA-B-HA can serve as a suitable carrier for the delivery for BMSC's.
9. Use of bovine hydroxyapatite may induce higher bioactivity than other forms of hydroxyapatite.

FUTURE WORK

The composites would be immersed in SBF to determine the bioactivity via ion exchange mechanisms. The total DNA content of the cells seeded on to 1:3 PLGA-B-HA composites would be analyzed and the results would be compared with 1:1 and 1:2 PLGA-B-HA composites. *In vivo* analysis would include subcutaneous implantation of macroporous, bioactive, 1:3 PLGA-B-HA composites loaded with bone marrow cells in rats.

REFERENCES

1. Khan MY., Katti DS. Katti, Laurencin CT. Novel polymer-synthesized ceramic composite-based system for bone repair: An *in vitro* evaluation. J Biomed Mater Res. 2004 Jun 15; 69A (4):728-737.
2. http://www.emedicine.com/orthoped/topic611.htm. Laurencin C, Yusuf K. 2005 Mar.
3. Calvert JW, Marra KG, Cook L, Kumta PN, DiMilla PA, Weiss LE. Characterization of osteoblast-like behavior of cultured bone marrow stromal cells on various polymer surfaces. J Biomed Mater Res. 2000 Nov; 52(2):279-84.
4. Francione GL. Xenografts and animal rights. Transplantation Proceedings. 1990; 22(3): 1044-1046.
5. Shi G, Cai Q, Wang C, Lu N, Wang S, Bei J. Fabrication and biocompatibility of cell scaffolds of poly (l-lactic acid) and poly (l-lactic-co-glycolic acid). Polymers for advanced technologies. 2002 Mar-Apr; 13(3-4): 227-232.
6. Rotter N, Aigner J, Naumann A, Planck H, Hammer C, Burmester G, Sittinger M. Cartilage reconstruction in head and neck surgery: comparison of resorbable polymer scaffolds for tissue engineering of human septal cartilage. J. Biomed. Mater. Res. 1998; 42:347-356.
7. Spain TL, Agrawal CM, Athanasiou KA. New technique to extend useful life of a biodegradable cartilage implant. Tissue Eng. 1998 Winter; 4(4): 343-52.

8. Aubin JE, Johan N.M. Heersche. Osteoprogenitor cell differentiation to mature bone-forming osteoblasts. Drug Dev Res. 49(3) :206 – 215.
9. Mankani MH, Kuznetsov SA, Fowler B, Kingman A, Robey PG. *In Vivo* Bone Formation by Human Bone Marrow Stromal Cells: Effect of Carrier Particle Size and Shape. Biotech. Bioeng. 2001 Jan 5; 72(1):96-107.
10. H. Ohgushi, Y. Dohi, T. Katuda, S. Tamai, S. Tabata, Y. Suwa. *In vitro* bone formation by rat marrow cell culture. J Biomed Mater Res. 1996 Nov; 32(3):333-40.
11. Karp JM, Shoichet MS, Davies JE. Bone formation on two-dimensional poly (DL-lactide-co-glycolide) (PLGA) films and three-dimensional PLGA tissue engineering scaffolds. J Biomed Mater Res. 2003 Feb; 64A (2): 388-396.
12. Panyam J, Williams D, Dash A, Pelecky D, Labhasetwar V. Solid-State Solubility Influences Encapsulation and release of Hydrophobic Drugs from PLGA/PLA Nanoparticles. J. Pharm. Sci. 2004; 93(7).
13. Ochi K, Chen G , Ushida T, Gojo S, Segawa K, Tai H, Ueno K, Ohkawa H, Mori T, Yamaguchi A, Toyama Y, Hata JI, Umezawa A. Use of Isolated Mature Osteoblasts in Abundance Acts as Desired-Shaped Bone Regeneration in Combination with a Modified Poly-DL-Lactic-Co-Glycolic Acid (PLGA)-Collagen Sponge. J Cell Physiol. 2003 Jan; 194(1):45-53.
14. Yang Q, Williams D, Owusu-Ababio G, Ebube NK, Habib MJ. Controlled release tacrine delivery system for the treatment of Alzheimer's disease. Drug Deliv. 2001 Apr-Jun; 8(2):93-8.

15. Abazinge M, Jackson T, Yang Q, Owusu-Ababio G. Comparison of *in vitro* and *in vivo* release characteristics of sustained release ofloxacin microspheres. Drug Deliv. 2000 Apr-Jun; 7(2):77-81.
16. Deng X, Hao J, Wang C. Preparation and mechanical properties of nanocomposites of poly (D,L-lactide) with Ca-deficient hydroxyapatite nanocrystals. Biomaterials 2001; 22(21): 2867-2873.
17. Murphy WL, Kohn DH, Mooney DJ. Growth of bone like mineral within porous poly (lactide-co-glycolide) scaffolds in vitro. J. Biomed Mater Res. 2000; 50(1):50-58.
18. Ambrosio AM, Sahota JS. Khan Y, Laurencin CT. An amorphous calcium phosphate polymer ceramic for bone repair. I. Synthesis and characterization. J. Biomed Mater. 2001; 58(3):295-301.
19. Liu C, Huang Y, Shen W, Cui J. Kinetics of hydroprecipitation at pH 10 to 11. Biomaterials. 2001 Feb; 22(4):301-6.
20. Borden MD, Attawia MA, Khan Y, Laurencin CT. Tissue Engineered microsphere-based matrices for bone repair and evaluation. Biomaterials 2002; 23(2):551-559.
21. Athanasiou KA, Zhu C, Lanctot DR, Agrawal CM. Fundamentals of biomechanics in tissue engineering. Tissue Eng 2000; 6(4):361-381.
22. Ripamonti U. Osteoinduction in porous hydroxyapatite implanted in heterotropic sites of different animal models. Biomaterials. 1996 Jan; 17(1):31-5.
23. Langer R. Drug delivery and targeting. Nature (6679S):5-10.

24. Bigi A, Boanini E, Panzavolta S, Roveri N, Rubini K. Bonelike apatite growth on hydroxyapatite-gelatin sponges from simulated body fluid. J Biomed Mater Res. 2002 Mar 15; 59(4):709-15.

25. Rogers KD, Daniels P. An X-ray diffraction study of the heat treatment on bone mineral microstructure. Biomaterials. 2002 Jun; 23(12):2577-85.

26. Yuan H, De Bruijn JD, Li Y, Feng J, Yang Z, De Groot K, Zhang X. Bone formation induced by calcium phosphate ceramics in soft tissue of dogs: a comparative study between porous alpha-TCP and beta-TCP. J Mater Sci Mater Med. 2001 Jan; 12(1):7-13.

27. Hartman EH, Vehof JW, Spauwen PH, Jansen JA. Ectopic bone formation in rats: the importance of the carrier. Biomaterials. 2005 May; 26(14):1829-35.

28. Vehof JW, van den Dolder J, de Ruijter JE, Spauwen PH, Jansen JA. Bone formation in CaP-coated and noncoated titanium fiber mesh. J Biomed Mater Res A. 2003 Mar 1; 64(3):417-26.

29. van den Dolder J, Vehof JW, Spauwen PH, Jansen JA. Bone formation by rat bone marrow cells cultured on titanium fiber mesh: effect of *in vitro* culture time. J Biomed Mater Res. 2002 Dec 5; 62(3):350-8.

30. Jansen JA, von Recum AF, van der Waerden JP, de Groot K. Soft tissue response to different types of sintered metal fibre-web materials. Biomaterials. 1992; 13(13):959-68.

31. Habibovic P, Yuan H, Valk CM, Meijer G, Blitterswijk CA, Groot K. 3D microenvironment as essential element for osteoinduction by biomaterials. Biomaterials 2005; 26:3565-3575.

32. Yuan H, Zou P, Yang Z, Zhang X, De Bruijn JD, De Groot K. Bone morphogenetic protein and ceramic-induced osteogenesis. J Mater Sci Mater Med. 1998 Dec; 9(12):717-21.

33. Urist MR, Lietze A, Dawson E. Beta-tricalcium phosphate delivery system for bone morphogenetic protein. Clin Orthop Relat Res. 1984 Jul-Aug ;(187):277-80.

34. Ono I, Ohura T, Murata M, Yamaguchi H, Ohnuma Y, Kuboki Y.A study on bone induction in hydroxyapatite combined with bone morphogenetic protein. Plast Reconstr Surg. 1992 Nov; 90(5):870-9.

35. Kai T, Shao-qing G, Geng-ting D. *In vivo* evaluation of bone marrow stromal-derived osteoblasts on calcium phosphate ceramic composites as bone graft substitutes in lumbar-intervertebral spinal fusion. Spine.2003 Aug 1; 28(15):1653-1658.

36. Ishaug SL, Crane GM, Miller JM, Yasko AW, Yaszemski MJ, Mikos AG. Bone formation by three-dimensional stromal osteoblast culture in biodegradable polymer scaffolds. J Biomed Mater Res. 1997 Jul; 36(1):17-28.

37. Thomson RC, Yaszemski MJ, Powers MJ, Mikos AG, Hydroxyapatite fiber reinforced poly (α-hydroxy ester) foams for bone regeneration. Biomaterials. 1998 Nov; 19(21):1935-43.

38. Miki T, Kozue M, Imai Y, Enomoto S. Experience with freeze-dried PLGA/HA/rh-BMP2 as a bone graft substitute. J Cranio-maxillofacial surgery (2000); 28: 294-299.

39. Yoneda M, Terai H, Imai Y, Okada T, Inoue H, Miyamoto S, Takaoka K. Repair of an intercalated long bone defect with synthetic biodegradable bone-inducing

implant. Biomaterials. 2005; 26: 5145-5152.

39. Kaito T, Myoui A, Takaoka K, Saito N, Nishikawa M, Tamai N, Ohgushi H, Yoshikawa H. Potentiation of the activity of bone morphogenetic protein-2 in bone regeneration by a PLA–PEG/hydroxyapatite composite. Biomaterials. 2005 Jan; 26(1): 73-79.

41. Ishii S, Tamura J, Furukawa T, Nakamura T, Matsusue Y, Shikiname Y, Okuno M. Long-Term Study of High-Strength Hydroxyapatite/Poly (l-lactide) Composite Rods for the Internal Fixation of Bone Fractures: A 2-4-Year Follow-Up Study in Rabbits. J Biomed Mater Res. 2003 Aug; 66(2): 539-547.

42. Ignatius AA, Betz O, Augat P, Lutz E. Claes. *In Vivo* Investigations on Composites Made of Resorbable Ceramics and Poly (lactide) Used as Bone Graft Substitutes. J Biomed Mater Res. 2001; 58(6): 701-709.

43. Ma PX, Zhang R, Xiao G, Franceschi R. Engineering new bone tissue *in vitro* on highly porous poly (α-hydroxyl acids)/hydroxyapatite composite scaffolds. J Biomed Mater Res. 2001 Feb; 54(2):284-93.

44. Tamai N, Myoui A, Tomita T, Nakase T, Tanaka J, Ochi T, Yoshikawa H. Novel hydroxyapatite ceramics with an interconnective porous structure exhibit superior osteoconduction *in vivo*. J Biomed Mater Res. 2002 Jan; 59(1): 110-117.

45. Hulbert SF, Morrison SJ, Klawitter JJ. Tissue reaction to three ceramics of porous and non-porous structures. J Biomed Mater Res. 1972 Sep; 6(5):347-74.

46. Flatley TJ, Lynch KL, Benson M. Tissue response to implants of calcium phosphate ceramic in the rabbit spine. Clin Orthop. 1983 Oct ;(179):246-52.

47. Yunhua H, David G, Winn RS, Hollinger JO. Fabrication of poly (hydroxy acid) foam scaffolds using multiple solvent systems. J Biomed Mater Res. 2002 Mar 5; 59(3):563-572.

48. Hua FJ, Kim GE, Lee JD, Son YK, Lee DS. Macroporous Poly (l-lactide) Scaffold 1. Preparation of a Macroporous Scaffold by Liquid-Liquid Phase Separation of a PLLA-Dioxane-Water System. J of Biomed Mater Res. 2002; 63(2): 161-167.

49. Zhang R, Ma PX. Poly (α-hydroxyl acids)/hydroxyapatite porous composites for bone tissue engineering. I. Preparation and morphology. J Biomed Mater Res. 1999 Mar 15; 44(4):446-55.

50. Nam YS, Park TG. Porous biodegradable polymeric scaffolds prepared by thermally induced phase separation. J Biomed Mater Res. 1999 Oct; 47(1):8-17.

51. Tadjoedin ES, de Lange GL., Bronckers JJ, Lyaruu DM, Burger EH. Deproteinized cancellous bone (Bio-Oss^{R}) as bone substitute for sinus floor elevation. J Clin Periodont. 2003 Mar; 30(3):261

52. Schwartz Z, Weesner T, van Dijk S, Cochran DL, Mellonig JT, Lohmann CH, Carnes DL, Goldstein M, Dean DD, Boyan BD. Ability of Deproteinized Cancellous Bovine Bone to Induce New Bone Formation. J Periodontol. 2000 Aug; 71(8):1258-69.

53. Xu H, Shimizu Y, Asai S, Ooya K. Grafting of deproteinized bone particles inhibits bone resorption after maxillary sinus floor elevation. Clin Oral Implants Res. 2004 Feb; 15(1):126-33.

54. Itala A, Nordstrom E, Ylanen H, Aro Hannu, Hupa M. Creation of microrough surface on sintered bioactive glass microspheres. J Biomed Mater Res 2001 Aug; 56(2):282-88.

55. NewView 5000 System Manual OMP-0471, Zygo® Corporation, Middlefield, CT.

56. Ranganathan Anand, Stephens L.S. Analysis of thrust surface sample with deterministic microasperities. 2003 Dec.

57. Thomson RC, Ysazemski MJ, Powers JM, Mikos AG. Fabrication of biodegradable polymer scaffolds to engineer trabecular bone. J Biomater Sci Polym Ed. 1995;7(1):23-38.

58. Ignatius AA, Betz O, Augat P, Claes LE. *In vivo* investigations on composites made of resorbable ceramics and poly (lactide) used as bone graft substitutes. J Biomed Mater Res. 2001; 58(6):701-709.

59. Hou Q, Grijpma DW, Feijen J. Porous polymeric structures for tissue engineering prepared by a coagulation, compression moulding and salt leaching technique. Biomaterials. 2003 May; 24(11):1937-1947.

60. Tu C, Cai Q, Yang J, Wan Y, Bei J, Wang S. The fabrication and characterization of poly (lactic acid) scaffolds for tissue engineering by improved solid-liquid phase separation. Polymers for advanced Tech. 2003 Aug; 14(8):565-573.

61. Rizzi SC, Heath DJ, Coombes AGA, Bock N, Textor M, Downes S. Bioegradable polymer/hydroxyapatite composites: Surface analysis and initial attachment of human osteoblasts. J Biomed Mater Res. 2001 Jun 15; 55(4):475-86.

62. Marra KG, Szem JW, Kumta PN, DiMilla PA, Weiss LE. *In vitro* analysis of biodegradable polymer blend/hydroxyapatite composites for bone tissue engineering. J Biomed Mater Res. 1999 Dec 5; 47(3):324-35.

63. Cui Y, Hou X, Qi AD, Wang HX, Wang H, Cai YK, Yin JY, Yao KD. Biomimetic surface modification of poly (L-lactic acid) with gelatin and its effects on articular chondrocytes in vitro. J Biomed Mater Res A. 2003 Sep 15; 66(4):770-8.

64. Steele JG, Johnson G, Mclean MK, Beumer JG, Hans JG. Effect of porosity and surface hydrophilicity on migration of epithelial tissue over synthetic polymer. J Biomed Mater Res. 2000 Jun 15; 50(4):475-82.

65. Borden M, Attawia M, Laurencin TC. The sintered microsphere matrix for bone tissue engineering: *in vitro* osteoconductivity studies. J Biomed Mater Res. 2002 Sep 5; 61(3):421-9.

66. Van Wachem PB, Beugeling T, Feijen J, Bantjes A, Detmers JP, Van Aken WG. Interaction of cultured human endothelial cells with polymeric surfaces of different wettabilities. Biomaterials 1985; 6:403-408.

67. Sato M, Slamovich EB, Webster TJ. Enhanced osteoblast adhesion on hydrothermally treated hydroxyapatite/titania/poly(lactide-*co*-glycolide) sol–gel titanium coatings. Biomaterials. 2005 Apr; 26(12):1349-57.

68. Schakenraad JM, Busscher JH, Wildevuur CR, Arends J. The influence of substratum surface free energy on growth and spreading of human fibroblasts in the presence and absence of serum proteins. J Biomed Mater Res 1986;20:773-784.

69. Van Kooten TG, Schakenraad JM, Vander Mei HC, Busscher JH. Influence of substratum wettability on the strength of adhesion of human fibroblasts. Biomaterials 1992; 13:897-904.

70. Fitton J, Dalton B, Beumer G, Johnson G, Griesser H, Steele J. Surface topography can interfere with epithelial tissue migration. J Biomed Mater Res. 1998 Nov; 42(2):245-57.

71. Stanford C, Keller J, Solursh M. Bone cell expression on titanium surfaces is altered by sterilization treatments. J Dent Res 1994; 73: 1061-1071.

72. Martin Y, Schwartz Z, Hummert T, Boyan B.D, Dean D, Cochran L, Simpson J. Effect of titanium surface roughness on proliferation, differentiation and protein synthesis of human osteoblast-like cells. J Biomed Mater Res 1995; 29:389-401.

73. Anselme K, Bigerelle M, Noel B, Dufresne, Judas D, Iost A, Hardouin P. Qualitative and quantitative study of human osteoblast adhesion on materials with various surface roughnesses. J Biomed Mater Res. 2000 Feb; 49:155-66.

74. Lossdorfer S, Schwartz Z, Wang L, Lohmann C, Turner J, Wieland M, Cochran D, Boyan B. Microrough implant surface topographies increase osteogenesis by reducing osteoclast formation and activity. J Biomed Mater Res. 2004 Sep 1; 70A:361-9.

75. Meyle J, Wolburg. Surface micromorphology and cellular interaction. J Biomater Appl 1993; 7:362-374.

76. Niederauer GG, McGee TD, Keller JC, Zaharias RS. Attachment of epithelial cells and fibroblasts to ceramic materials. Biomaterials 1994; Apr; 15(5):342-52.

77. Redey SA, Nardin M, Bernache-Assolant D, Rey C, Delannoy P, Sedel L, Marie PJ. Behavior of human osteoblastic cells on stoichiometric hydroxyapatite and type A carbonate apatite: role of surface energy. J Biomed Mater Res 2000; 50:353-64.

78. Durucan C, Brown PW. Low temperature formation of calcium-deficient hydroxyapatite-PLA/PLGA composites. J Biomed Mater Res. 2000 Sep 15; 51(4):717-25.

79. Oreffo ROC, Driessens FC, Planell JA, Triffitt JT. Growth and differentiation of human bone marrow osteoprogenitors on novel calcium phosphate cements. Biomaterials. 1998;19:1845-1854.

80. http://www.waichung.demon.co.uk/webanim/OsteWeb.htm**.** University of Glasgow. 1996.

VITA

Harini Raman was born in Mumbai, India in 1980. She attended the University of Mumbai in 1997 where she received her Bachelors of Science in Biomedical Engineering in 2001. In 2002 she was offered the task of lecturing senior year students in Instrumentation and control engineering in India. She came to the United States in 2002 to pursue her Master's degree in biomedical engineering at the University of Texas at Arlington. In 2003 she was working as a summer intern at the University of Kentucky. Following this year, she continued her Master's in Biomedical Engineering at the University of Kentucky. As a graduate student, she presented her research work at the Society for Biomaterials conference in Philadelphia, PA.